5-2013

Fast Pyrolysis of Muconic Acid and Formic Acid Salts

Laura Duran
University of Maine - Main

FAST PYROLYSIS OF MUCONIC ACID AND FORMIC ACID SALTS

by

Laura Duran

A Thesis Submitted in Partial Fulfillment
of the Requirements for a Degree with Honors
(Chemical Engineering)

The Honors College

The University of Maine

May 2013

Advisory Committee:

Adriaan R. P. van Heiningen, Ober Professor of Chemical Engineering, Advisor
William J. DeSisto, Associate Professor of Chemical Engineering
Brian G. Frederick, Associate Professor of Chemistry
Robert Glover, Professor of Political Science, Honors College
M. Clayton Wheeler, Associate Professor of Chemical Engineering

Abstract

Lignocellulosic biomass is emerging as a sustainable resource for the production of alternative liquid fuels. As the need to lessen dependence on petroleum sources grows, lignocellulosic feedstocks are being investigated as a renewable, abundant source of energy. Chemical pulping processes include a high-lignin by-product, black liquor, which is already used for fuel in industry. Black liquor is burned to generate steam and electricity and to recover pulping chemicals. Currently, the thermochemical conversion of black liquor to liquid fuel is being researched at The University of Maine. In this black liquor research, an intermediate lignin-derived acid, muconic acid, and formic acid are forming. Formic acid has been integral in thermal deoxygenation (TDO) and fast pyrolysis studies at The University of Maine. TDO is the pathway by which neutralized carboxylic acids, which can be derived from lignocellulosic feedstocks, have been observed to condense and deoxygenate to produce cyclic and aromatic molecules. Since alkaline pulping chemicals present in black liquor neutralize acids to form salts, the salts can be studied using TDO and fast pyrolysis. Thermal decomposition products of sodium muconate and a mixture of sodium muconate and sodium formate, were analyzed using Py-GC/MS. This technique provides a qualitative understanding of the volatiles present after fast pyrolysis of muconate and muconate/formate mixtures. In this study, the optimal fast pyrolysis conditions for salt volatilization and decreased carbonaceous residues were found to be approximately 500°C with formate present. Major products identified were aromatics (indene, cresol, phenol, toluene, and other substituted benzenes), unsaturated hydrocarbon chains (C_6-C_9), cyclopentanones and cyclopentenones.

To my family, friends, and mentors.

Acknowledgements

This project was made possible by the DOE EPSCoR award # DE-FG02-07ER46373. A special thanks to Jamie St. Pierre, who assisted with experimental set-up, data interpretation, and advice along the way. Thank you to Dr. van Heiningen for advising. Thank you to Paige Case, who assisted with Py-GC/MS data acquisition and set-up.

Table of Contents

List of Figures and Tables

Introduction

U.S. consumption of motor gasoline, jet fuel and distillate fuel oil fell from 20.8 million bbl/day in 2005 to 18.6 million bbl/day in 2012 as consumers and industries managed fuel use and switched to natural gas as it became less expensive.[1] As society shifts toward non-petroleum fuel sources, there is a need for alternative fuels, especially from carbon-neutral, renewable sources.

Biomass is considered to be the only carbon-neutral, sustainable source for liquid fuel production.[2] Lignin is nature's only renewable aromatic source, and is the second most abundant biomass component on Earth.[3] Lignocellulosic feedstocks, which include, wood, agricultural residue and switchgrass, are 15 to 30 weight percent lignin.[4] The U.S. Department of Energy foresees forestland and cropland resources providing 1.3 billion dry tons/year of biomass. The DOE also expects that most of the biomass will be used by the forest products and food processing industries.[5]

The pulp and paper industry generates black liquor, a lignin-containing by-product stream during pulping, which is burned as fuel. Black liquor dry solids from Kraft pulping have a higher heating value (HHV) of approximately 13.5-15.5 MJ/kg dry solids.[6] An intermediate during black liquor oxidation is muconic acid. This project investigates the thermal decomposition products of muconic acid salts, as well as muconic acid and formic acid salt mixtures, to understand whether it is possible to convert the compounds present in partially oxidized black liquor to a renewable fuel by thermal deoxygenation (TDO).

Current Uses of Muconic Acid

The need to decrease petroleum usage and dependence is an issue across many industries. Plastic producers are looking for alternatives to petroleum-based sources. Products like nylon-6,6, polyurethane, and polyethylene terephthalate (PET) are derived from adipic acid. Adipic acid can be synthesized from benzene (Figure 1) and muconic acid.[7] Metabolic engineering research is being conducted to understand muconic acid's potential as a platform chemical for consumer bio-plastics.[8] Muconic acid can be converted via hydrogenation to produce nylon and polyurethanes, or converted via Diels-Alder reactions with acetylene to terephthalic acid, a component of PET (Curran). Some yeasts and bacteria have natural capabilities of producing muconic acid. *E. coli* was found to produce muconic acid from glucose (Curran).

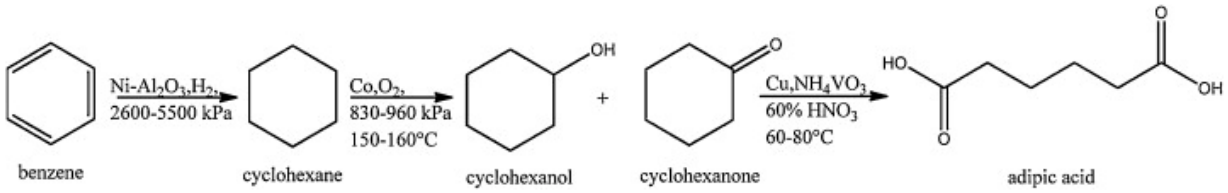

Figure 1. Synthesis of adipic acid from benzene.[7]

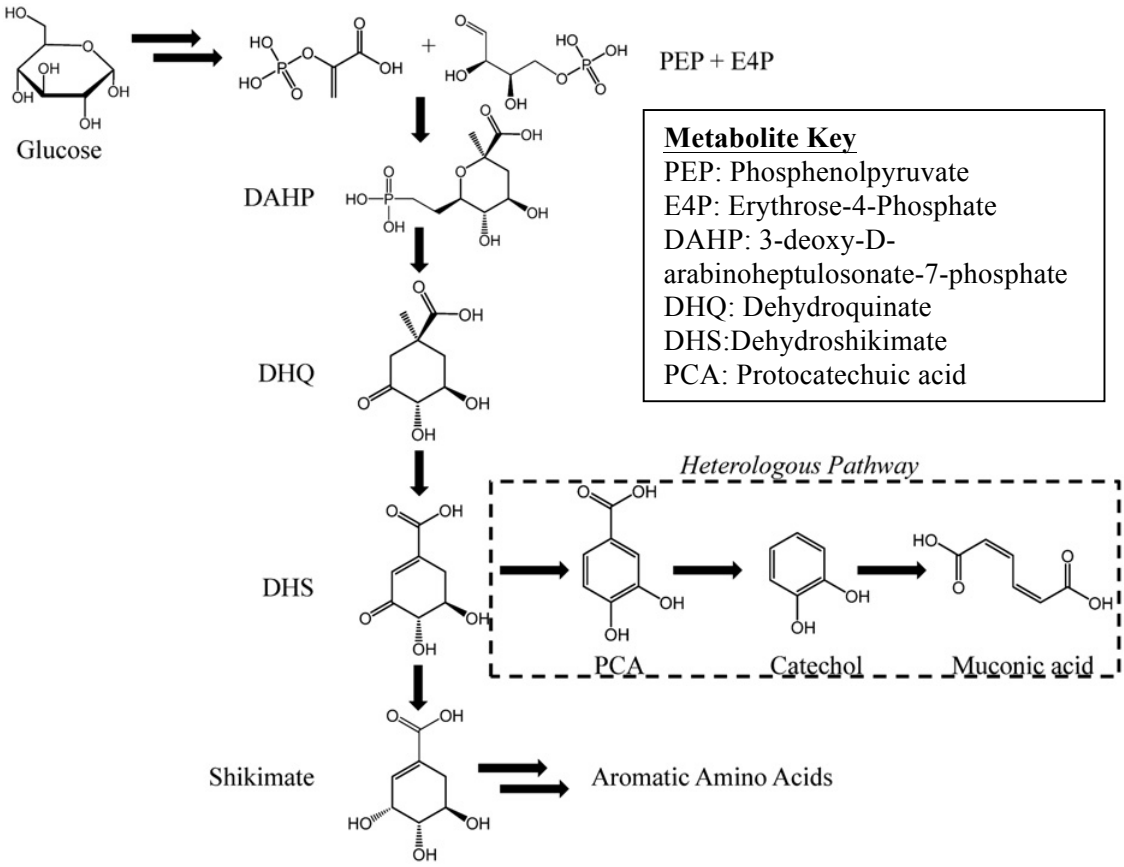

Figure 2. Muconic acid production pathway depicted in the context of the shikimate pathway in yeast.[8]

The generation of muconic acid from lignin-derived aromatics or from sugars will not be explored further in this study, but is mentioned to give potential uses of muconic acid as a specialty chemical product.

Chemical Pulping Overview

In the pulp and paper industry, lignin is already used as a fuel source. Lignin and hemicellulose are separated from cellulose in chemical pulping and ends up in a by-product stream, black liquor, which is subsequently burned for its energy density (~13.5-15.5 MJ/kg dry solids).[6] The major steps of Kraft pulping are detailed in Figure 3.

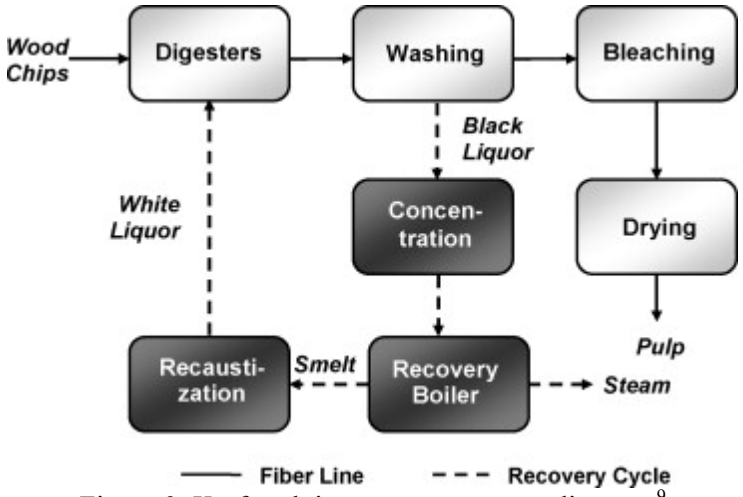

Figure 3. Kraft pulping process concept diagram.[9]

In Kraft pulping, the raw materials, wood chips and sawdust, are digested into pulp using white liquor, which contains sodium hydroxide (NaOH) and sodium sulfide (Na_2S). In an alternative process, soda-AQ pulping, wood chips are cooked in the presence of a small amount of anthraquinone (AQ). Thus, AQ replaces the function of sodium sulfide, and the resulting black liquor does not contain sulfur. In Kraft cooking, 92-94% of lignin is removed.[10] Pulp is separated from the residual liquor, known as black liquor, in brown stock washing. Pulp passes through "countercurrent vacuum drum washers" aligned in series to displace black liquor without significant liquor dilution.[11] After brown stock washing, multiple-effect evaporators concentrate weak black liquor (approximately 15% solids) into heavy black liquor (70-75% solids).

Heavy black liquor travels to the recovery boiler, where it is burned to generate steam and electricity. Recovery is an essential step in the Kraft process for providing steam and electricity for mill use, and for chemical recovery. Smelt also leaves the recovery boiler, and is dissolved to produce green liquor. Green liquor, which consists of sodium carbonate and sodium sulfide is converted into white liquor using burned lime, which is produced in the

lime kiln.

Muconic Acid in Lignin Oxidation

Residual lignin not removed in digestion is removed during delignification and bleaching stages. Oxygen in an alkaline medium delignifies the black liquor.[12] Muconic acid-type structures appear as intermediates in oxygen delignification. During this stage, "the most reactive sites in lignin are the phenolic structures, more specifically their phenolate forms in the alkaline solution."[12] Oxygen delignification reactions involving phenolates form a muconate with a propane side chain (Figure 4.)

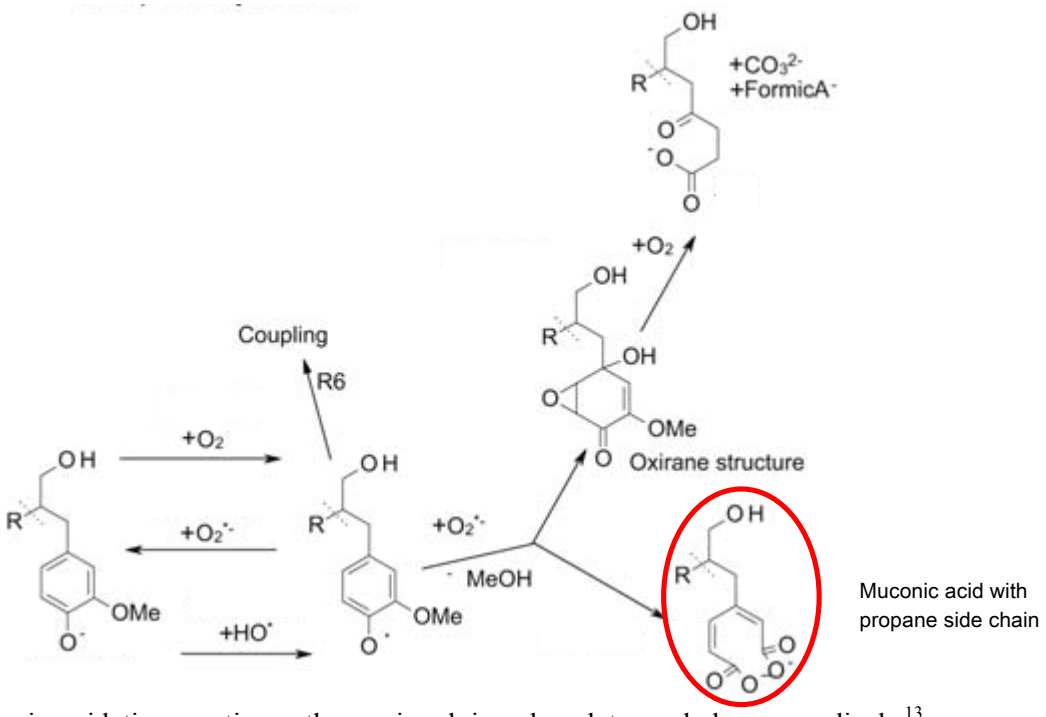

Figure 4. Lignin oxidation reaction pathways involving phenolates and phenoxy radicals.[13]

In Figure 4, a guaiacyl phenolate reacts with oxygen to form radicals.[13] Under alkaline conditions, the guaiacoxy radical reacts with a superoxide anion radical and water and via ring opening forms muconic acid with a propane side chain. Methanol is also

liberated during this step (Kuitunen).

Nonphenolic, phenolic and condensed phenolic guaiacyls can react with hydroxide ions to produce ortho-quinones via an alternative pathway.[13] The o-quinone reacts with a hydroperoxyl radical (HO_2^-) to form muconate with a propane side chain (Figure 5).

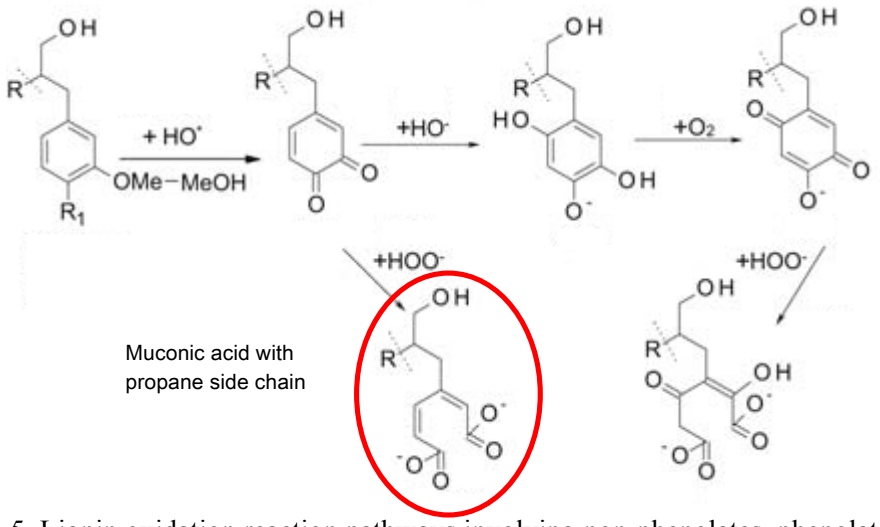

Figure 5. Lignin oxidation reaction pathways involving non-phenolates, phenolates, and condensed phenolic guaiacyls.[13]

Upon further degradation, muconic acid-type structures from either pathway react with hydroxide ($HO^{\bullet}$) or superoxide ($O_2^{\bullet}$) radicals to form maleic acid with a propane side chain, carbonate, formate and oxalate.[13] Degradation continues as these products react with hydroxide or superoxide radicals to form pentanoic acid (Figure 6).

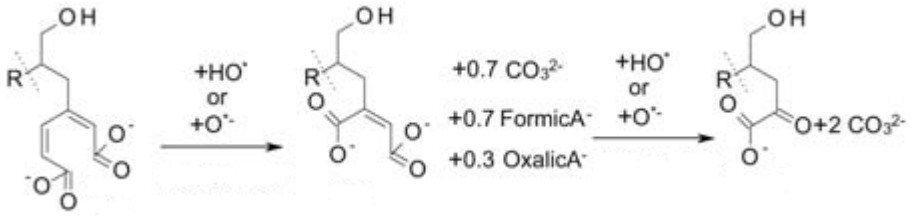

Figure 6. Reaction pathway for degradation of aliphatic organic compounds following lignin oxidation.[13]

Muconic acid-type structures are expected to be a major intermediate in oxygen delignification or black liquor oxidation in the laboratory, based on literature. The purpose of this project is to gain a better understanding of the behavior of decomposition products present in black liquor as it is oxidized and subsequently thermally deoxygenated. Muconic acid is used as a lignin-based model compound with or without the presence of formic acid. After neutralization to their sodium salts, the pyrolysis behavior of the dry solids is studied on a micro-scale through Py-GC/MS.

Why Add Formate?: TDO and FAsP

Formic acid has been shown to increase the liquid yield and energy density of bio-oils produced via fast pyrolysis and thermal deoxygenation (TDO) at The University of Maine.[14-15]

Thermal deoxygenation was first researched by Schwartz et al. using levulinic acid, an organic acid derived from acid hydrolysis of cellulose in the "Biofine" process.[16] The acid was neutralized with calcium hydroxide, and then heated between 350-450°C.[2] In TDO, the calcium levulinate is "simultaneously condensed and deoxygenated" to form cyclic and aromatic molecules. When pure levulinic acid underwent TDO, cyclization and dehydration compounds were observed, as well as 1,2-dimethylcyclopentane. Calcium appears to facilitate ketonic decarboxylation while acting as a base.

The products were found to have low oxygen to carbon ratios.[2] Low oxygen to carbon ratios are key in liquid fuel analysis, as biomass has an O:C of approximately 0.5, while gasoline has an O:C of zero. While levulinic acid esters have energy densities around

26 MJ/kg, the TDO products had an energy density of 35 MJ/kg. TDO products can be upgraded to drop-in fuels via hydrogenation using Ru and Pt catalysts. After catalytic hydrogenation, the liquid would need refining as is done in petroleum processing.

In addition to levulinic acid, acid hydrolysis of cellulose via the "Biofine" process produces formic acid in a 1:1 molar ratio with levulinic acid. Since one of the decomposition products of formate salts is known to be hydrogen,[17] their effect on TDO was studied by Case et al. Once again, the acids were neutralized with calcium hydroxide.[14] TDO oils with formate/levulinate molar ratios ranging from 0-1.5 were produced and analyzed. The optimal quality and yield were discovered at a 1:1 formate/levulinate ratio. The products of pure calcium levulinate TDO were water-soluble cyclic ketones with an energy density of 35 MJ/kg. The 1:1 formate/levulinate TDO oil had more desirable fuel properties. The oil was water insoluble, so it separated easily from the aqueous phase. Increasing the formic acid concentration yielded more conjugated double bond behavior, according to ^{13}C NMR studies. These products are predicted to be aromatics or olefins.

Thermal deoxygenation proceeds through ketonic decarboxylation reactions and deoxyhydrogenation at atmospheric pressure.[14] Neither catalyst, nor external hydrogen supplies are required. For the TDO oil produced with formate, the organic phase had a neutral pH, and the energy density was greater than 40 MJ/kg.

Similar benefits were observed for fast pyrolysis oils produced with the addition of formate.[15] When lignin was pyrolyzed by itself, "highly oxygenated phenols" were produced as identified by gas chromatography/mass spectrometry (GC/MS) analysis. The oxygen content remained high (O:C ratio of 0.19), and the HHV was 30.7 MJ/kg. Calcium formate

addition provided an *in situ* source of "reactive" hydrogen that aided in deoxyhydrogenation. Bio-oil from lignin/calcium formate mixtures contained alkylated phenols and fewer "methoxy/hydroxyl functionalities."[15] Increasing the ratio of formate to lignin increased aromatics in the oil, according to carbon-13 nuclear magnetic resonance (^{13}C NMR) data. The most favorable result was a bio-oil with a 1:1 formate/lignin mass ratio, an O:C ratio of 0.067, and a HHV of 41.7 MJ/kg.

The TDO and FAsP methods are potentially attractive, because no catalyst is necessary for oil production. Formic acid salts can be added for pyrolysis, or used in the mixture with levulinic acid salts derived from acid hydrolysis of cellulose. Both exhibit that the addition of formic acid salts decreases the oxygen content and increases the HHV. Moreover, char formation decreases, so carbon ends up in the liquid product, and not in solid carbonaceous material.

Other organic acids derived from biomass, such as muconic acid, were proposed to be suitable for energy densification via TDO.[2] The organic acid functional groups, once neutralized with alkali (alkaline earth) metal hydroxides, should form deoxygenated and energy densified products at temperatures between 400-600°C.

Salt Sample Synthesis

The muconic acid and formic acid salt mixtures studied in this project were prepared at The University of Maine. Trans-trans muconic acid purchased from Sigma Aldrich (98% pure) was neutralized with sodium hydroxide (Fisher, 98.9% pure) to form sodium muconate. In preparation, the muconic acid was dissolved in ethanol, as it is not soluble in water, to make solution A1. A sodium hydroxide pellet was crushed and dissolved in

deionized (DI) water to make solution A2. The two solutions were mixed to produce solution A. For muconate/formate samples, sodium formate purchased from Fluka Analytical (99.0% pure) was dissolved in DI water to make solution B. Solutions A and B were mixed to form solution C at room temperature. Solution C was evaporated until dry in a vacuum oven. If only sodium muconate was being prepared, only solution A was dried in a vacuum oven.

In these experiments, the salts were prepared with known stoichiometric proportions. For the sodium mixtures, muconate and formate were present in a 1:2 molar ratio, respectively. This is important to note for pyrolysis and oxidation data analyses. See Appendix A for synthesis data.

Py-GC/MS Overview

Pyrolysis is the heating of organic material in the absence of oxygen. As heat energy is applied, the starting material forms volatilized fragments that can be detected using gas chromatography-mass spectrometry (GC/MS). This is a common analytical technique for identifying individual volatile compounds in a mixture. For GC/MS combined with micro-scale pyrolysis, the solid samples are pyrolyzed in a quartz tube. For this project, a CDS Pyroprobe 5000 and Shimadzu GCMS-QP2010S were used.

Pyrolysis vapors pass through a heated transfer line into the GC injector. When a sample is injected into the instrument, it first passes through a chromatographic column. This column is a coiled, long capillary silica tube. The tube is internally coated with polar or nonpolar material. For this experiment, the column's coating was 5% polar (diphenyl polysiloxane), and 95% nonpolar (dimethyl polysiloxane). The sample adsorbs to the

coating. As the GC oven temperature rises, molecules desorb from the coating. Desorption occurs when the oven temperature reaches the molecule's boiling point. Carrier gas then transports the molecules through the column. Helium was the carrier gas in these experiments. Once compounds volatilize and pass through the entire column, they enter the MS interface.

A mass spectrometer is comprised of an ionization chamber, an analyzer and an ion detector. As molecules elute from the GC into the MS, they are "bombarded" with electrons or charged molecules in the ionization chamber.[18] The ions move into the analyzer, which is under vacuum, and pass through a quadrupole created within 4 parallel rods. This quadrupole is electrically charged. A radio frequency signal, whose DC/AC amplitudes are varied linearly, control the mass and resolution of ions that pass through the filter. Ions with different mass-charge ratios, or *m/z*, travel through the analyzer and enter the detector one at a time one. The mass spectrum displays ions that reach the detector according to their *m/z* ratio.

In the detector, ions are deflected onto a plate. For each ion, a signal is sent to the GC/MS software as "an ion current versus *m/z* versus time."[17] The sum of the raw signal is plotted against time to form a TIC, or total-ion chromatogram. GC/MS data include three variables: signal intensity, mass-charge ration, and time. Signal intensity is a dependent variable, while mass-charge ratio and time are independent variables. One ion's *m/z* can be extracted to plot a single-ion chromatogram (SIC). Both the TIC and mass spectrum are used for chemical identification. In this experiment, the GC/MS software, GCMS Solution, matched NIST library data with mass spectra results to identify compounds. The software

also evaluated each match's similarity to NIST library data and reported a match percentage. Reports obtained through GCMS Solution were used for volatile compound analysis.

Oxidation and Carbonate Reactions

Sodium formate is known to decompose to hydrogen, carbonate and carbon monoxide after reaching 300-400°C,[18] as shown in:

$$2NaHCOO \rightarrow Na_2CO_3 + H_2 + CO \quad (1)$$

It is hypothesized that "reactive" hydrogen assists in the deoxygenation essential for TDO and FAsP. Sodium carbonate is expected to remain in the quartz tube after pyrolysis while volatile compounds enter the GC/MS. Carbonate is expected in muconate decomposition as well. Based on prior TDO studies, it has been hypothesized that sodium carbonate will form after fast pyrolysis in this project, as the temperature ranges and conditions are similar to the work of Schwartz *et al*. and Case *et al*.

Carbonaceous char was seen after TDO of calcium formate/levulinate, and was expected in the present experiment.[14] To quantify the carbonaceous material produced by pyrolysis, the sample tube is placed in a 550°C muffle furnace for oxidation. Changes in mass before and after oxidation are assumed to be solely caused by solid carbon reacting with oxygen to form carbon dioxide:

$$C\ (s) + O_2 \rightarrow CO_2 \quad (2)$$

Sodium carbonate will not decompose when the oven temperature is kept below 600°C. The sodium carbonate mass can be calculated as the residual mass after carbonaceous material oxidation. This is a hypothesis, and was tested in experimentation. (See Experimental Procedure and Results.) The following reaction depicts sodium carbonate

decomposition at very high temperatures.

$$Na_2CO_3 \rightarrow Na_2O + CO_2 \quad (3)$$

Experimental Procedure

A quartz tube was used for all pyrolysis trials. Before each trial, the tubes were cleaned with acetone, dried with compressed air, and cleaned again with the pyroprobe clean function. In pyroprobe cleaning, the probe hung on the outside of the instrument. While the tube rested in the filament, it was heated to 1000°C for 5.00 seconds. Any vapors produced were released to the environment. If solids could still be seen in a previously used tube after one round of cleaning, the tube was cleaned until the solids were no longer present.

After cleaning, the tube was weighed. One third of the tube was then stuffed with quartz wool. The tube was weighed again before the salt sample was loaded. The tube was weighed again with the sample inside. Finally, another third of the tube was stuffed with quartz wool so the sample was sandwiched between two wool sections. The fully packed tube was weighed. When blanks were run, the tube was either empty or two thirds of the tube was stuffed with quartz wool.

The tube was carefully inserted into the pyroprobe. Before the trial began, the carrier gas (He) purge flow rate was measured with a Restek Pro Flow 6000 flow meter. The purge flow rate was kept at approximately 1.00 mL/min to ensure a uniform residence time for all trials. A dial on the front of the pyroprobe was used to control the flow rate.

All trials were performed at pyroprobe temperatures of 550°C, 600°C, or 650°C for 15.00 seconds. According to the CDS manual, and Nowakowski et al., there is "a temperature difference of 100°C between the coil and the sample temperature." Thus, the

salt temperatures reach 450°C, 500°C, or 550°C, respectively. The temperatures 450°C, 500°C, or 550°C will be used for all further analysis and discussion.

These temperatures were chosen based on thermogravimetric analyses (TGA) of both salts. Slow pyrolysis was performed in a TA Instruments Q500-130S TGA. Nitrogen was used as the sweep gas. The TGA temperature was ramped 10°C/min from 20°C to 700°C, as indicated by Figure 7, and Appendix B.

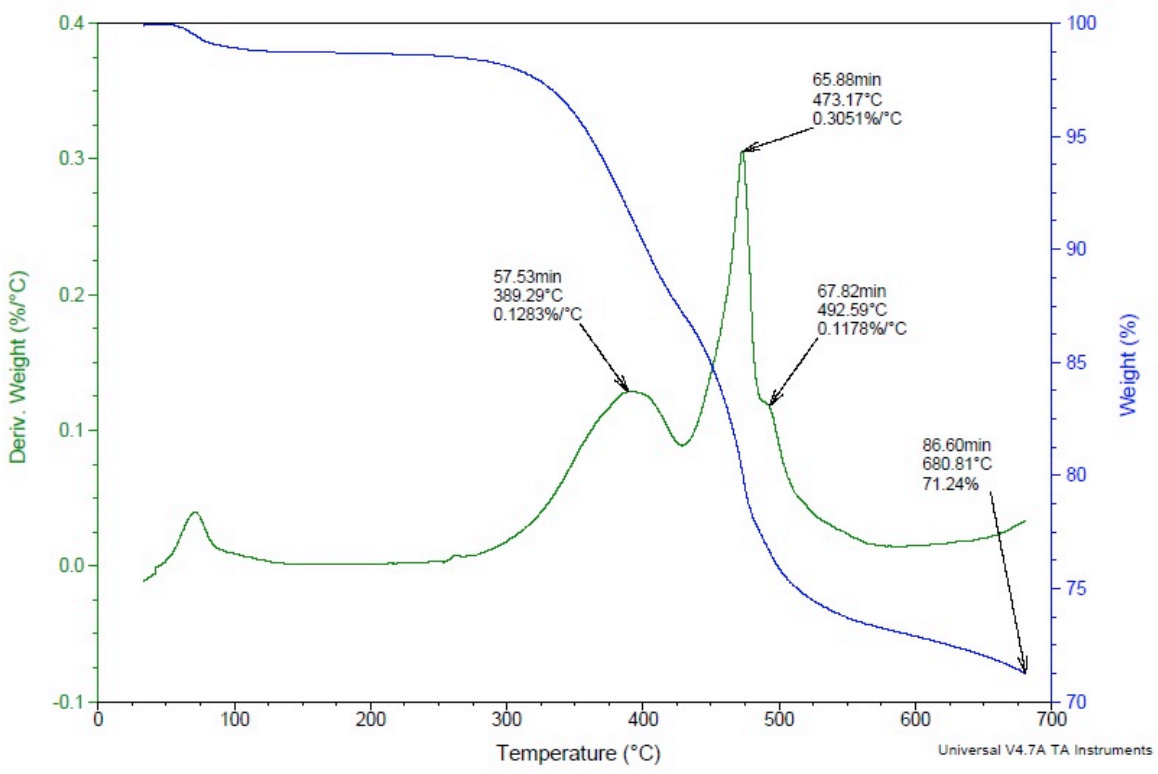

Figure 7. Slow pyrolysis of sodium muconate/formate in a TGA with decomposition peaks indicated. Temperature was ramped at 10°C/min from 20°C to 700°C. N_2 was used as the sweep gas.

Fast pyrolysis temperatures were chosen from decomposition peaks seen in the TGA plots. For sodium muconate, a major peak in the rate of mass loss is seen just below 500°C

(Appendix B). In the sodium muconate/formate plot, decomposition appears at 389°C, 473°C and 492°C. Based on peaks seen in Figure 7, it can be assumed that decomposition of sodium muconate and sodium muconate/formate occurs between 450-550°C. By 550°C, most decomposition appears to be complete. The same pyroprobe temperatures were used for both samples for comparison. Temperatures much higher than 450°C and 500°C are not used, as volatiles other than carbon dioxide and water are desired as products. As seen in Figure 8, all or most of the decomposition of sodium formate, sodium muconate, and sodium muconate/formate occurred at or below 550°C, which was the highest pyrolysis temperature in these experiments.

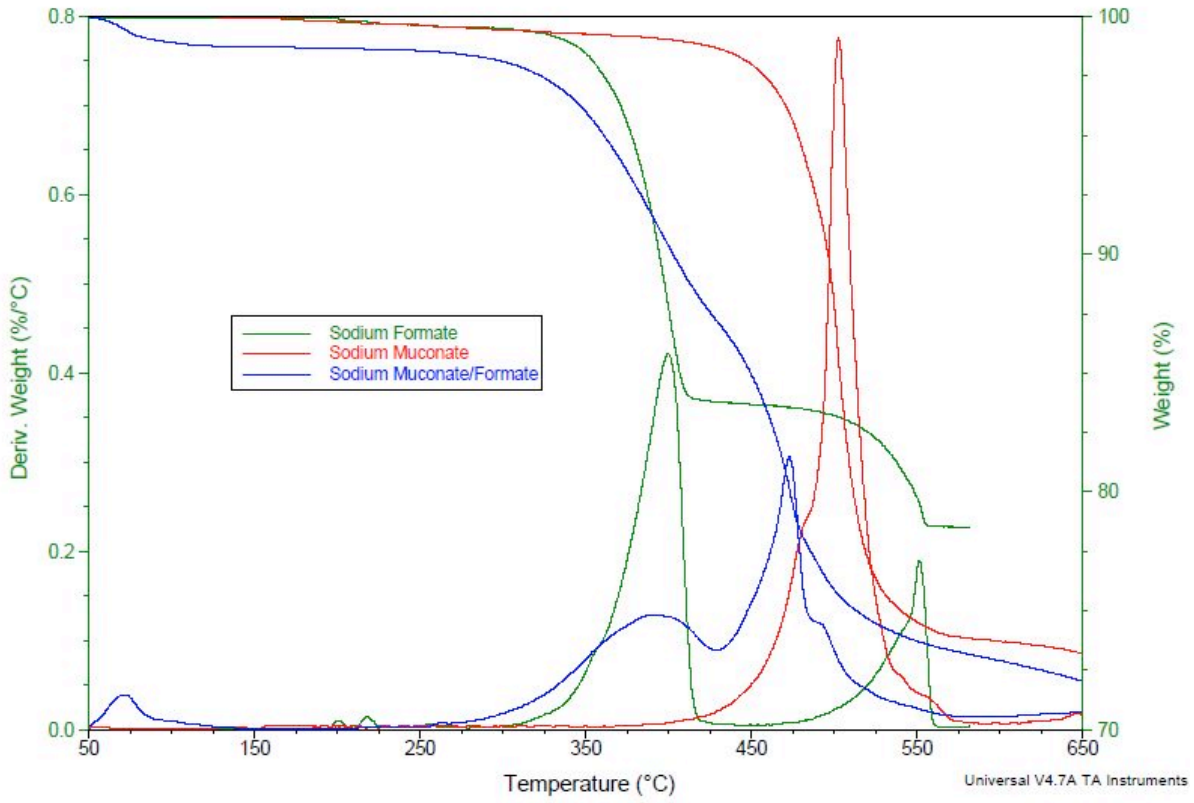

Figure 8. Slow pyrolysis of sodium formate, sodium muconate and sodium muconate/sodium formate in a TGA. Temperature was ramped at 10°C/min from 20°C to 700°C. Temperature was

only ramped to 600°C for sodium formate. N_2 was used as the sweep gas.

The pyroprobe temperature was set for 15.00 seconds with no gradual increase; the temperature increased instantaneously from room temperature (25°C) to the program setting. The GC/MS program was designed to separate non-polar compounds. Aromatics were expected to form as the muconate was assumed to react with "reactive" hydrogen released during formate decomposition, and potentially form ring structures. Thus, the oven temperatures ramp relatively slowly between 120-160°C. The GC/MS conditions are listed in Table 1.

Table 1. Py-GC/MS conditions and program for sodium muconate and sodium muconate/formate experiments.

GC Conditions		**MS Conditions**	
Column Oven Temp	40.0 °C	Ion Source Temp	260 °C
Injection Temp	250.0 °C	Interface Temp	280 °C
Pressure	49.5 kPa	Solvent Cut Time	0 min
Total Flow	24.0 mL/min	Start m/z	35.00
Column Flow	1.0 mL/min	End m/z	450.00
Linear Velocity	36.1 cm/s	Total time	87.07 min
Purge Flow	1.0 mL/min		
Split Ratio	20.0 : 1		
Carrier Gas	He		

GC Oven Program
1. Hold at 40.0°C for 1.00 min.
2. Ramp at 2.00°C/min for 40.0 min.
3. Hold at 120.0°C for 2.00 min.
4. Ramp at 1.50°C/min for 26.7 min.
5. Hold at 160.0°C for 2.00 min.
6. Ramp at 25.00°C/min for 5.40 min.
7. Hold at 295°C for 10.00 min.

After pyrolysis, the sample is transferred to a crucible and cooled in a desiccator. Since the tube remains in the pyroprobe as the 87-minute program completes, its temperature is above room temperature. (The transfer line remains at 300°C, and the pyroprobe heater remains at 300°C during the program.) The tube is weighed once it has cooled to room temperature. This measured mass, which represents the mass lost during pyrolysis, is referred to as volatilized mass, or volatiles. A Denver Instruments PI-225D scale was used.

To quantify the masses of carbonaceous material and sodium carbonate that remain in the tube, after the loss of volatiles, the tube is brought to a 550°C muffle furnace (Thermolyne 62700) for oxidation in one hour increments. The sample is oxidized for one hour, allowed to cool, and then weighed. The tube remains in a crucible, and is cooled in a desiccator. This process is repeated until consecutive masses are within 0.02 mg of each other. If this cannot be achieved within the first three or four hours of oxidation, the tube is left in the furnace overnight.

To verify the mass of carbonate in the tube after oxidation, and to compare experimental to theoretical carbonate masses, sodium concentration was tested. The sodium concentration was determined by the Plant, Soil and Environmental Sciences Department at The University of Maine. In preparation, the quartz wool and product remaining after oxidation were transferred to a vial. A solution was prepared by adding 0.1 M HCl, which dissolved sodium possibly bound to the quartz wool. The quartz wool was filtered out using a nitrocellulose filter (0.45 μm) in filter housing. The solution was dried overnight in a Fisher ISOTEMP Oven 200 Series at 110°C.

The complete list of equipment used is in Table 2.

Table 2. Equipment summary for Py-GC/MS, oxidation and mass measurements.

Balance	Denver Instruments PI-225D
Pyroprobe	CDS Pyroprobe 5000
GC/MS	Shimadzu GCMS-QP2010S
Muffle Furnace	Thermolyne 62700 Furnace (550°C)
Oven	Fisher ISOTEMP Oven 200 Series (110°C)
Flow Meter	Restek Pro Flow 6000

Results

Blanks consisting of empty quartz tubes and quartz tubes stuffed with quartz wool underwent pyrolysis at three temperatures (450°C, 500°C and 550°C). Mass before and after pyrolysis was measured. Blank tube trials were run in duplicate. Tubes used for the second 450°C and 500°C trials also underwent oxidation for one hour in a 550°C muffle furnace. (Oxidation was not originally included in blank trial procedures, but was added.) Both 550°C trials included oxidation. The mass after oxidation was greater, and closer to the mass before pyrolysis, than the mass after pyrolysis. For the tube pyrolyzed at 450°C and oxidized, the first and final recorded masses were the same. This is seen in Figure 9.

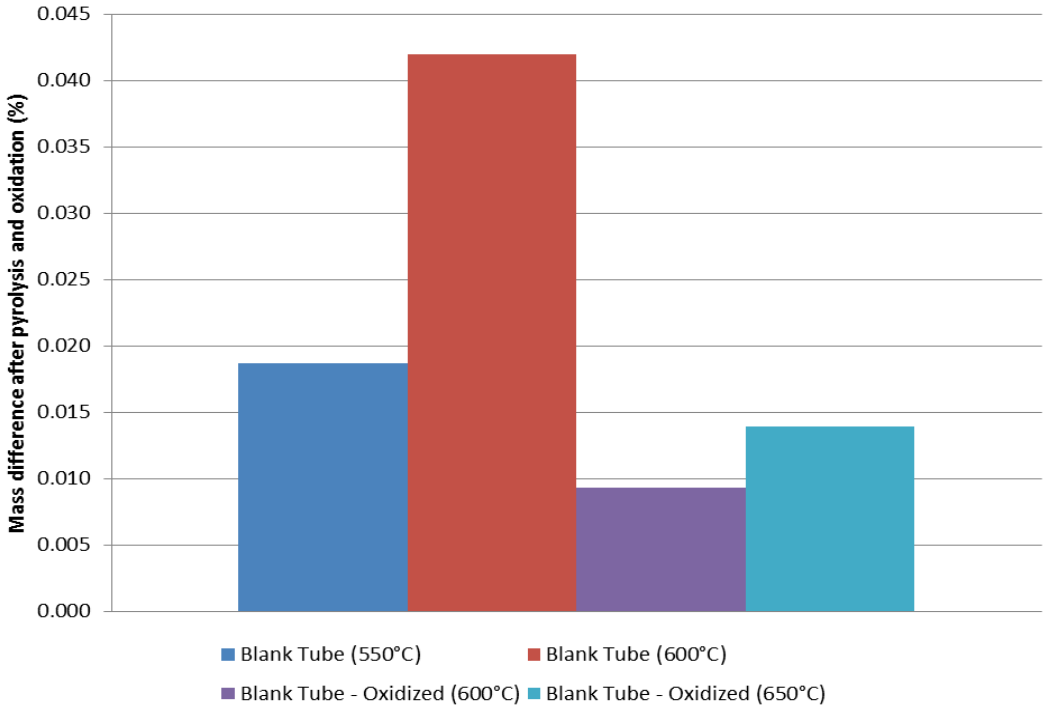

Figure 9. Mass differences of empty quartz tubes after pyrolysis at 450°, 500°C or 550°C and oxidation at 550°C. Blank Tube – Oxidized (600°C) was not duplicated. The blank tube pyrolyzed at 550°C and oxidized had no overall change in mass.

For the tubes stuffed with quartz wool, the same procedure was followed. Two pyrolysis trials were completed. The second of the 450°C and 500°C trials also included oxidation, while both 550°C trials included oxidation, as shown in Figure 9. Since the mass differences seen in empty blank tubes were all under 0.05%, even when considering error, the effect of tube mass differences was neglected when calculating volatilized mass by difference. Mass difference represents the difference between initial and final mass (after pyrolysis) as a percentage of the initial mass. However, the mass difference percentages for tubes stuffed with quartz wool were accounted for in calculations. Quartz wool masses are known from pre-pyrolysis measurements. From these measurements, 7.67%, 2.67%, and 4.99% of quartz wool masses are assumed to be lost during 450°C, 500°C, and 550°C

pyrolysis trials, respectively. This affects the calculations used to determine estimated salt mass volatilized in pyrolysis. The volatilized salt mass is assumed to be the difference between total mass lost after pyrolysis and the estimated quartz wool mass lost after pyrolysis.

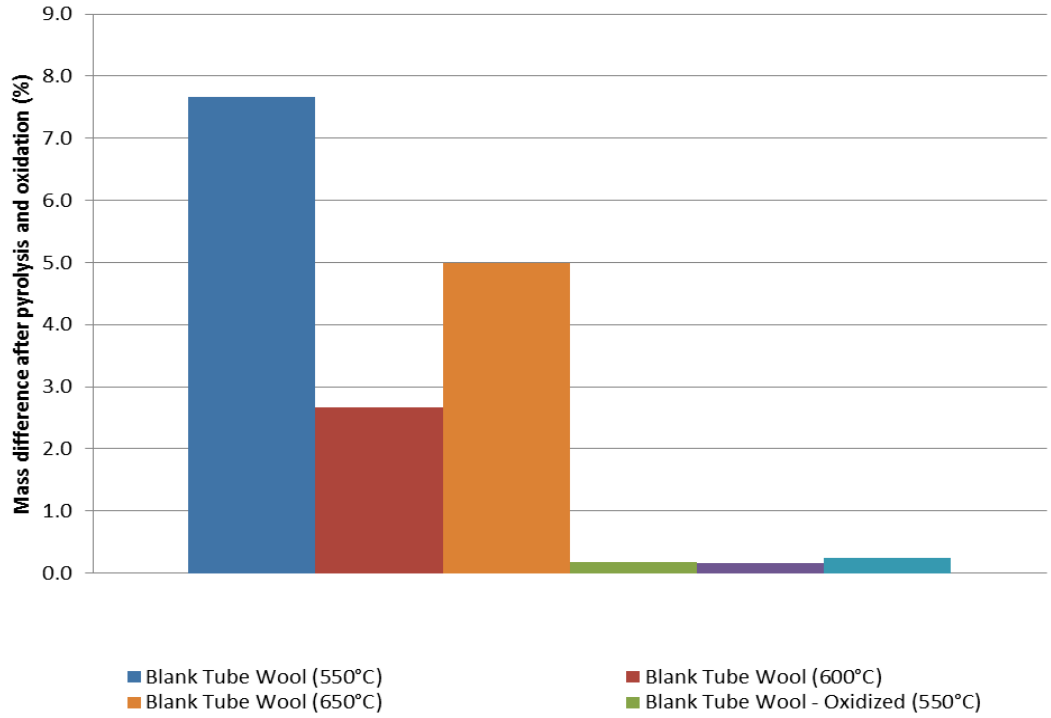

Figure 10. Mass differences of quartz tubes stuffed with quartz wool after pyrolysis at 450°, 500°, or 550°C and pyrolysis with oxidation.

Mass Balances

Mass balances were performed based on masses taken before and after pyrolysis and after oxidation. Figure 11 shows the average mass contributions for each salt at all temperatures. All trials were run in duplicate. Mass percentages are based on the original mass of salt used for pyrolysis. The 550°C trials showed an increase in volatilized mass from 12.9% to 21.1%, and a decrease in carbonaceous material from 43.5% to 27.5% when formate was present. Similarly, the 600°C trials exhibit a rise in volatilized mass from

26.6% to 30.0%, and a decrease in carbonaceous material from 26.7% to 18.6% when formate was present in the mixture. However, the volatilized mass percentage was the same for 550°C trials when considering error. The amount of carbonaceous material in the 550°C trials decreased from 33.2% to 11.0% with the addition of formate, though. These data suggest an optimal temperature for fast pyrolysis of muconic acid salts of approximately 500°C with formate present, based on volatile yield.

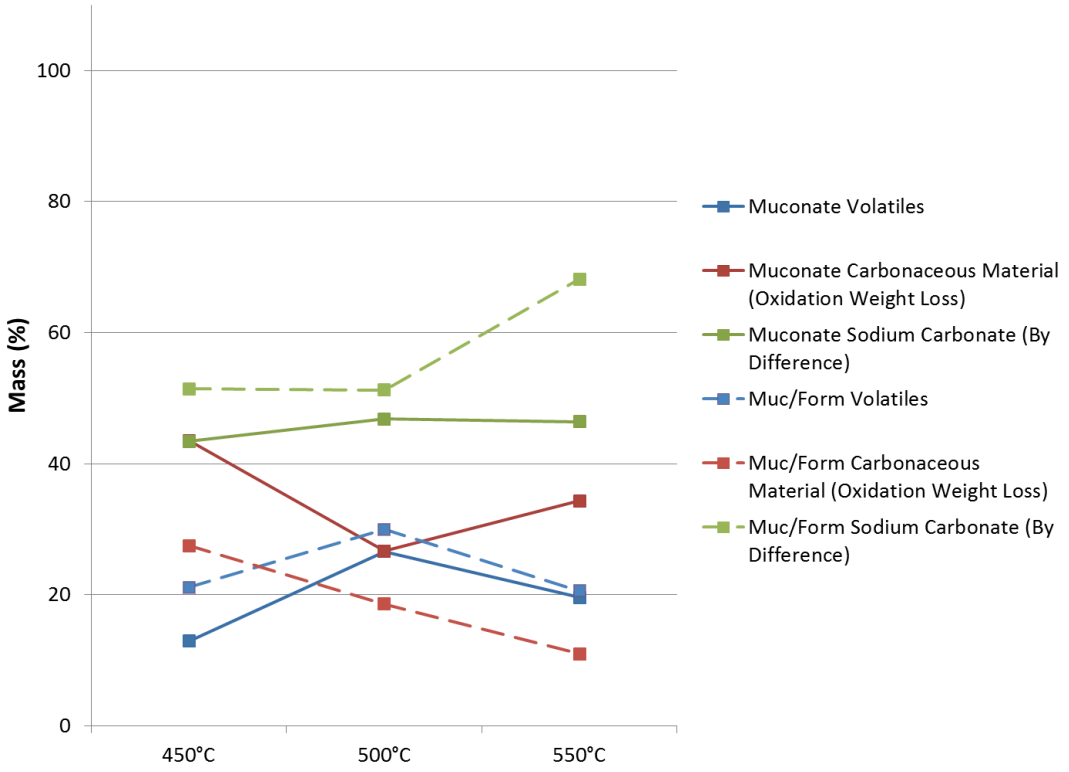

Figure 11. Mass balances for sodium muconate and sodium muconate/formate fast pyrolysis trials.

While it cannot be seen in Figure 11, percent difference is represented in the above figure, as well as all following figures illustrating trial data. Percent difference is graphically expressed with error bars, and represents the difference between two data points as a percentage of the average.

Product Distributions

Shimadzu analysis software, GCMS Solution, was employed to classify volatilized products into major categories. The chromatogram for sodium muconate/formate 450°C Trial 11 exemplifies the types of compounds analyzed and categorized using Py-GC/MS (Figure 12).

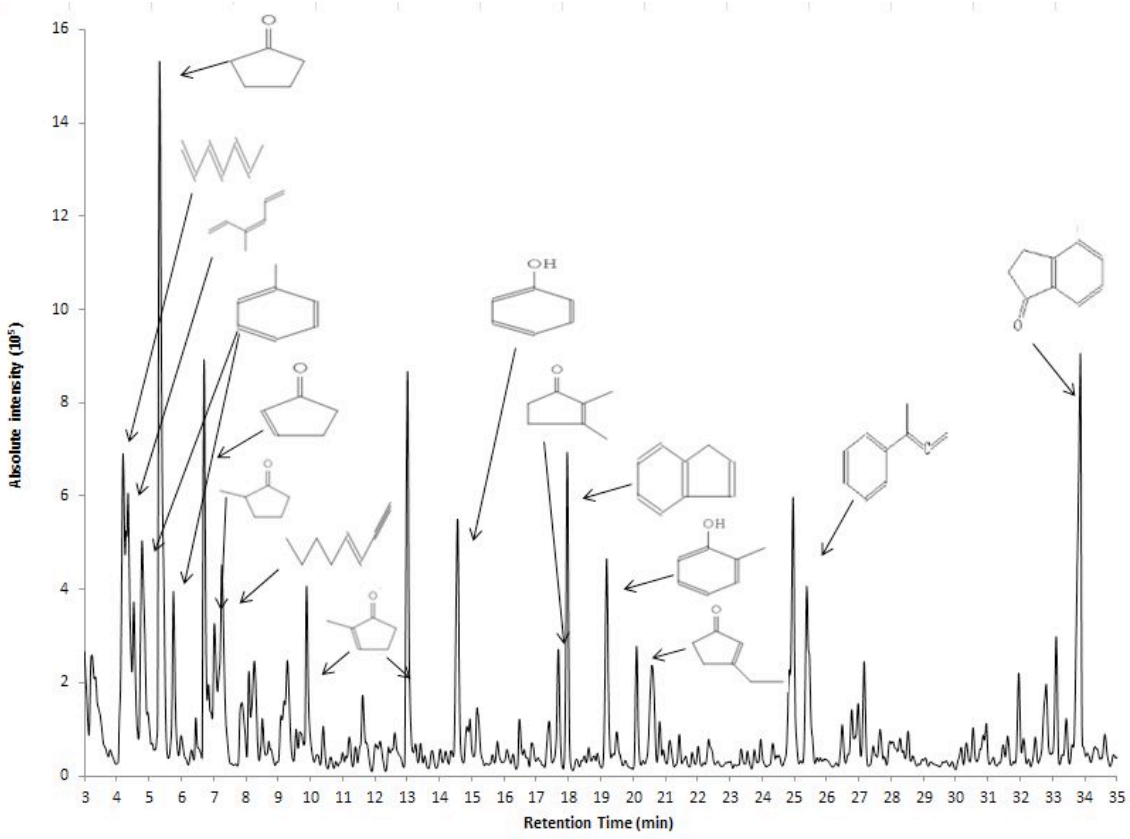

Figure 12. Sodium muconate/formate 450°C Trial 11 chromatogram with major products and indicated peaks.

As seen in Figure 13, the product distribution varied between individual trials, while categories of compounds remained relatively consistent throughout all trials. The mass spectra data for the top twenty peaks by chromatographic peak area were collected, analyzed and filtered for each trial based on functional group similarities. Results that included

compounds or atoms assumed to be absent in the Py-GC/MS system, such as bromine or boron, were excluded. Thus, the results were normalized while including compounds containing carbon, hydrogen and oxygen only. Results from blank experiments were analyzed, and were determined to be column bleed-off. The peaks appeared at retention times greater than 70 minutes, which was above the retention times for the major peaks in salt pyrolysis trials, and included compounds related to siloxane, the column's coating.

"Unknown" results could not be obtained from GCMS Solution. "Other" products were classified for some muconate 500°C Trial 13, muconate/formate 400°C Trials 10 and 13, and muconate 550°C Trials 22 and 24 results. These included a cyclopropane substituted with alkenes and a cyclopentene derivative for muconate/formate 400°C Trial 10. An isopropyl methyl ketone and a cyclohexene derivative were observed for muconate/formate 400°C Trial 13. Muconate 550°C Trial 22 results included tetracyclododeca-3,8-dien-11-one, bicycloundeca-1,3,5,7,9-pentaene, and o-biphenylenemethane. Muconate 550°C Trial 24 contained 1-methyl-2-cyclohexen-1-ol and azulene in its data. Also, muconate 550°C Trial 22 was the only trial to have xylenol, a cyclohexane diol and dimethyl phenyl ethanol in its matches.

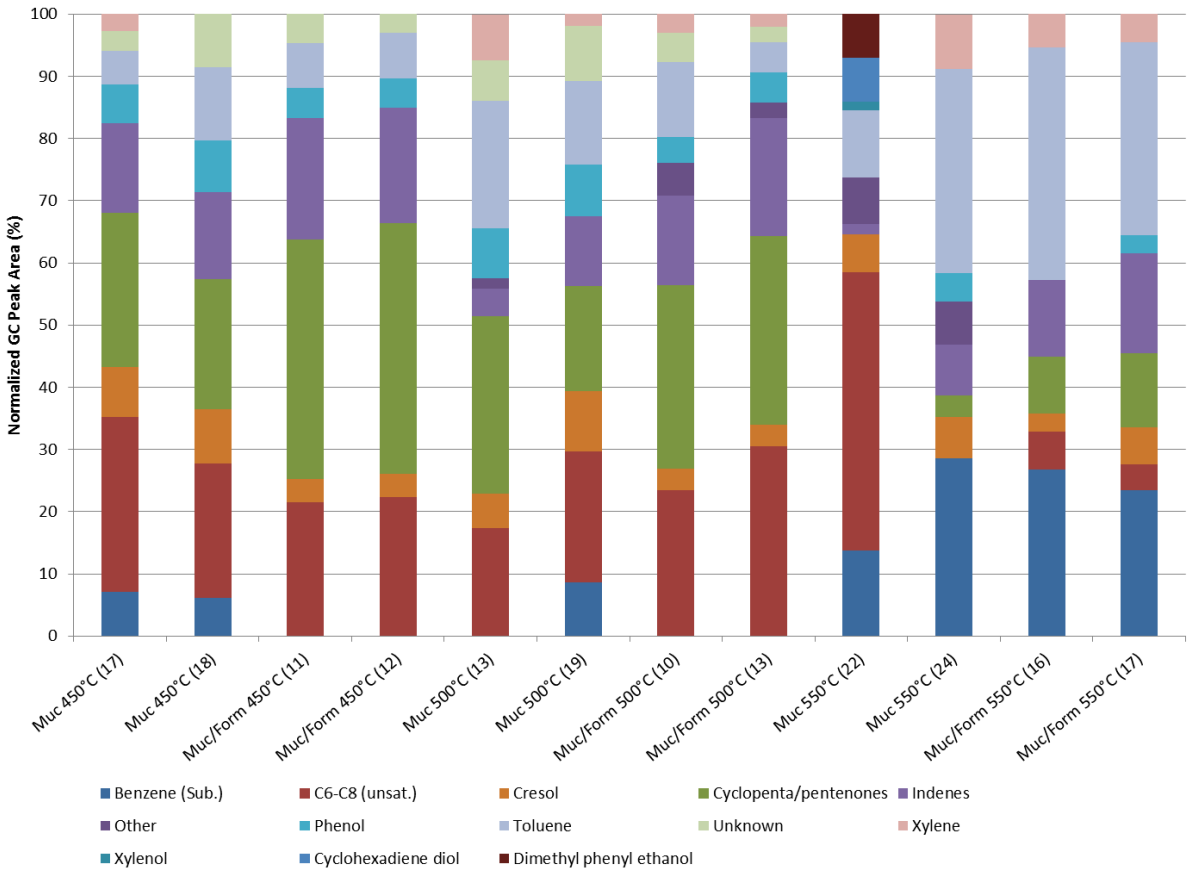

Figure 13. Compound product distributions by trial for sodium muconate and sodium muconate/formate.

Product distribution trends were analyzed using the major product categories seen in GC/MS results. Similar to mass balance results, trends mostly correlate to the presence or absence of formate. The benzene (sub.) category was only found in the pure sodium muconate trial results at 450°C and 500°C, as seen in Figure 14. This category includes benzenes substituted with groups containing more than one carbon. For example, ethylbenzene and 1-methylene-2-propynyl benzene are seen in muconate 450°C Trials 17 and 18. Muconate 500°C Trial 19 included 1-methyl-1,2-propadienyl benzene and 1–methyl-2-butynyl benzene. Muconate and muconate/formate 550°C trials included a

significantly higher amount of benzene (sub.) compounds. An average 28.6% area for muconate and 25.1% for muconate/formate was found. Since the data from muconate 550°C Trial 22 appeared inconsistent, compared to all other trials, they were not included in product distribution analysis.

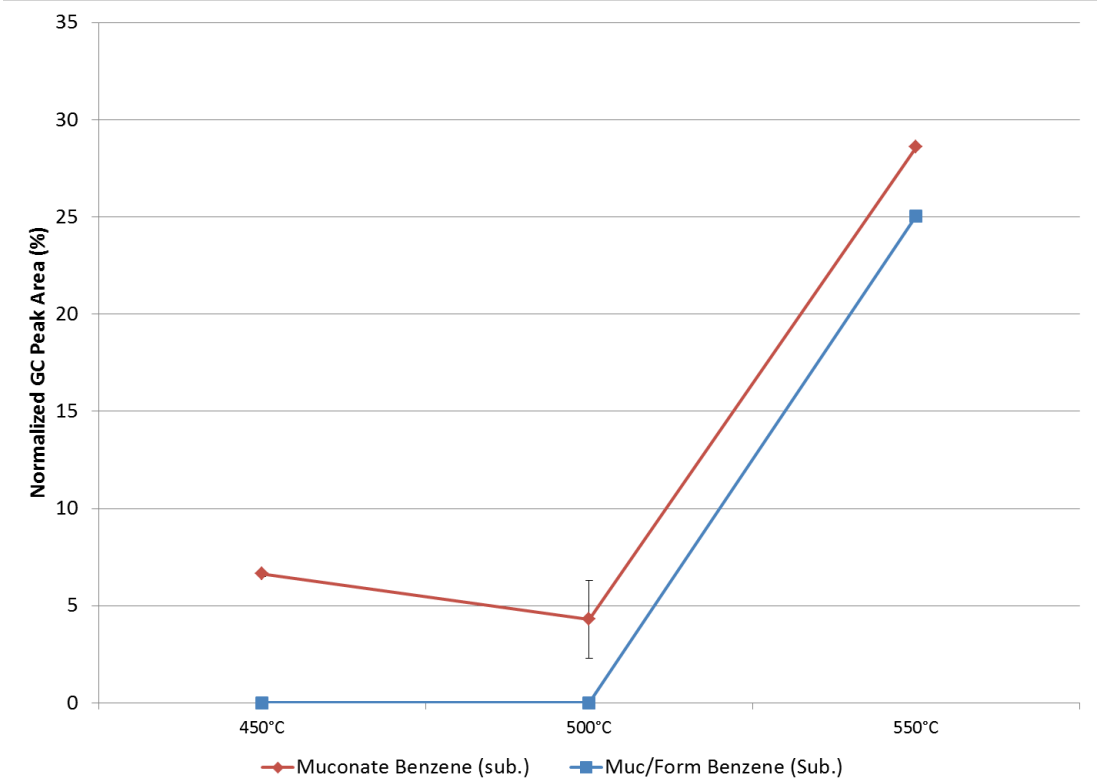

Figure 14. Benzene (sub.) product trends from fast pyrolysis of sodium muconate and sodium muconate/formate.

Cresol and phenol quantities decreased with formate present for 450°C and 500°C trials. Cresol contribution changed from approximately 8% to 4%. Phenol decreased from around 7-8% to 5% for 550°C and 600°C trials, while remaining at about 2% for all 550°C trials. Indenes increased with formate only at 450°C and 550°C. Indenes include unsubstituted indene, methylated indene, and inden-1-one. (See Appendix E for product

distribution figures.)

Cyclopenta/pentenones also increased with formate present at 450°C. The 550°C results show a significant decrease in cyclopenta/pentenones. The lower temperature trials had cyclopenta/pentenone area percentages of at least 20%. While cyclopenta/pentenones increase from 1.8% to 10.5% with formate present in 550°C data, the area percentages are relatively low. Conversely, toluene increases to 32.8% for muconate, and 34.1% for muconate/formate in 550°C results. This is much higher than the 7.3-17.0% range observed for the lower temperature trials. The increase in benzene (sub.) compounds, toluene, and the decrease of cyclopenten/pentenones at 550°C represents a rise in aromatic hydrocarbons and a decrease in compounds with one oxygen atom. However, the unsaturated C_6-C_9 hydrocarbon chains, decrease in abundance as temperature increases. Overall, the pyrolysis products only contain unsaturated hydrocarbons, or cyclic organic compounds with a single oxygen atom—at any temperature and regardless of the presence of formate.

Sodium Sources

The mass remaining in the pyrolysis tube after oxidation is assumed to be sodium carbonate and quartz wool. See Appendix F for stoichiometric calculations based on one mole of sodium carbonate forming for each mole of sodium muconate, and two moles of sodium carbonate forming for every one mole of sodium muconate in the muconate/formate salt mixture.

The increase in theoretical sodium carbonate with the presence of formate mirrors the increase in experimental carbonate (Figure 15). In the mass balances, this corresponded to increased volatile matter and decreased carbonaceous material. The theoretical carbonate

increase also meets expectations set by TDO and FAsP; adding formate aids in deoxygenation by forming water vapor and minimizes carbonization.

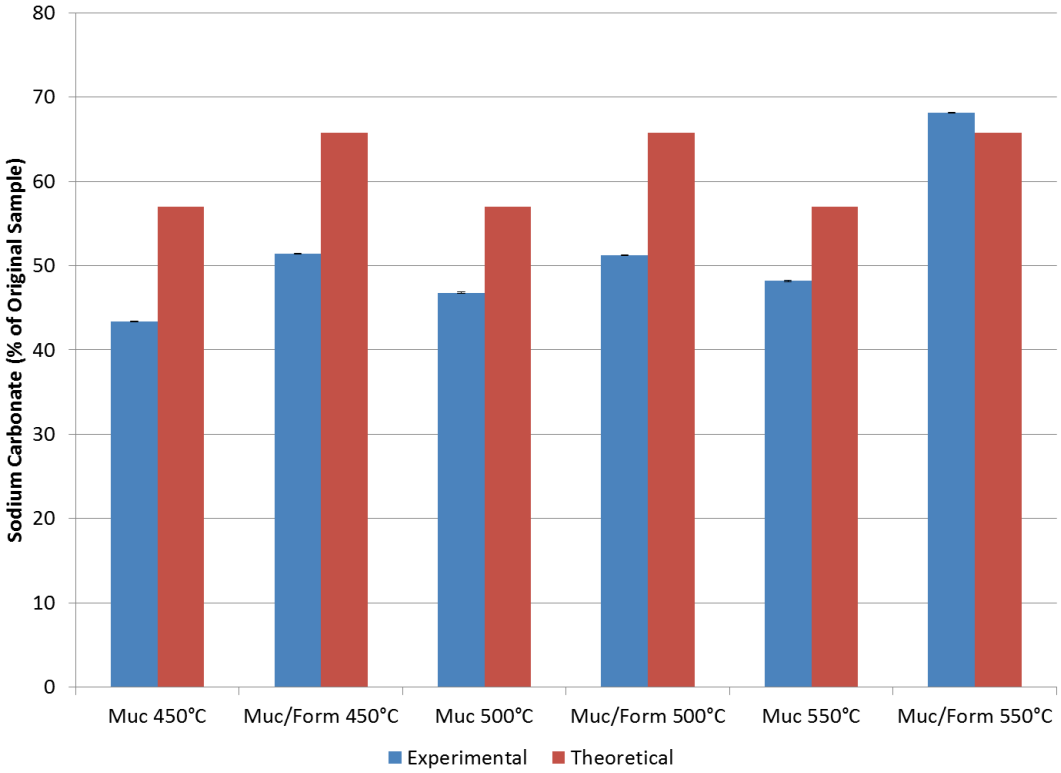

Figure 15. Mass percentage of sodium carbonate present in samples of sodium muconate and sodium muconate/formate after fast pyrolysis and oxidation. Experimental results were calculated by difference of the tube mass before and after pyrolysis, and after oxidation. Theoretical percentages are calculated based on stoichiometric ratios of carbonate formation upon starting material decomposition, assuming sodium carbonate is the only solid product remaining after oxidation.

Figure 15 also shows that for all trials except muconate/formate 550°C, the experimental sodium carbonate was found to be lower than theoretical sodium carbonate. This suggests that there may be a loss of sodium during pyrolysis, or that sodium is in another form than sodium carbonate in the final product. Two samples that were run at 500°C, sodium muconate Trial 19 and sodium muconate/formate Trial 13, were taken to the Department of Plant, Soil and Environmental Sciences Laboratory. These were samples that

after oxidation that were filtered to remove quartz wool, as explained in the Experimental Procedure section. The sample after oxidation and experimental sodium carbonate masses for sodium muconate 500°C trial 19 are not identical because the entire sample after oxidation was not able to be transferred to a vial for sodium concentration analysis. Table 3 shows that the theoretical carbonate mass calculated using concentration data determined in the laboratory was greater than the mass of sample after oxidation. Again, this supports that another sodium compound exists in the final product.

Table 3. Experimental and theoretical sodium carbonate masses after pyrolysis and oxidation.

	Mass (mg)				
Trial	Original Salt	Sample After Oxidation	Experimental Sodium Carbonate	Theoretical Sodium Carbonate by Stoichiometry	Theoretical Sodium Carbonate by Sodium Analysis
Na Muconate 500°C (19)	1.67	0.72	0.76	0.95	0.75
Na Muc/Form 500°C (13)	1.27	0.67	0.67	0.84	**0.90**

Sodium hydroxide may be present in the product remaining after fast pyrolysis and oxidation as unreacted material from salt synthesis, or as a decomposition product. To assess this hypothesis, residual effective alkali (REA) was tested using the sodium muconate/formate Trial 15 sample, which was run at 550°C. A pH meter was calibrated with standard buffer solutions of pH 7.00 and pH 10.00. The sample after oxidation, including the quartz wool, was dissolved in 10 mL of DI water. The pH of this solution was 9.97. If the pH is at or below 11.3, the REA is zero. This suggests that there may have been no sodium hydroxide present, but it is also likely that the sample was too dilute to determine the

REA.

Compounds other than sodium carbonate may be contributing to the sodium product. However, these compounds cannot be analyzed based on the data in Table 3. Since theoretical sodium carbonate mass calculated by sodium analysis for muconate/formate 500°C Trial 13 is greater than the experimental and theoretical sodium carbonate mass by stoichiometry, no conclusive trend can be seen. More sodium concentration analysis is necessary to understand the discrepancy between theoretical and experimental sodium carbonate masses. TIC, or a combination of TC and TOC, could be used to determine the amount of carbon in a sample. Additional 550°C muconate/formate trials should be performed to further explore if experimental sodium carbonate is less than, equal to or greater than theoretical carbonate at those conditions.

Relation of Results to TDO and FAsP

The major pyrolysis products were cyclic compounds, except for unsaturated C_6-C_9 chains. This was expected based on the open ring structure of muconic acid-type structures found during lignin oxidation.[13] Cyclopentanones and cyclopentenones were expected, as they contain fewer carbons than the starting salt, and have been seen in TDO products.[14] "The aqueous phase" of calcium levulinate/formate TDO oil "was found to contain hydrocarbon products, such as methyl-cyclopentenones, also found in TDO of pure levulinic acid."[14]

Figure 16 provides a potential reaction pathway from sodium muconate to sodium carbonate and cyclopentenone. In this pathway, one of the carbonyl groups cleaves from the chain with another oxygen and sodium. The oxygen and sodium from the other end of the

chain also cleave, and a sodium carbonate is formed. This would leave C_2 and C_6 at the ends of the chain, which would form a five-carbon ring. If the C_2-C_3 double bond became saturated, only one carbon-carbon double bond would remain in the cyclopenteneone. This would require a source of "reactive" hydrogen (H_2). Sodium formate may provide this hydrogen if it is present in the salt mixture.

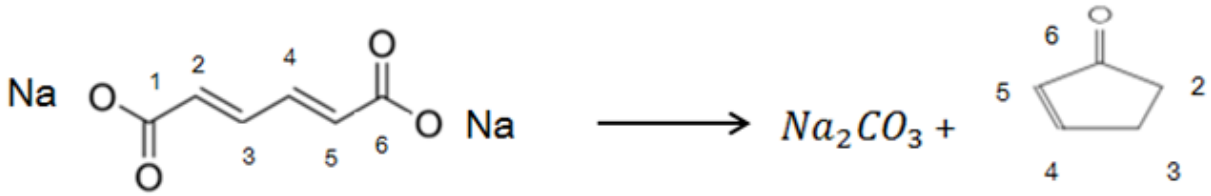

Figure 16. Potential reaction pathway for cyclopentenone from muconic acid during fast pyrolysis from 450-550°C.

In previous fast pyrolysis studies, GC/MS analysis of oil produced from pure lignin showed oxygenated phenols.[15] Oil pyrolyzed with a lignin/calcium formate mixture showed alkylated phenols. While phenols were present in the volatile product distribution in this project, cresol—the only alkylated phenol from the data—decreased when formate was added for 450°C and 500°C trials. Additionally, ^{13}C NMR analysis illustrated aromatics increasing with increased formate addition.[15] However, according to normalized GC peak area percentages shown in Figures 13, a trend for the relative abundance of aromatics cannot be discerned due to error. Similar product distributions, especially including aromatics, were seen in TDO, FAsP and this project, but there do not seem to be conclusive trends at this time.

Conclusion

Py-GC/MS results suggest that fast pyrolysis of neutralized muconic acid and formic

acid salts will produce mostly cresol, phenol, toluene, indene, cyclopentanones, cyclopentenones, benzene substituted with chains containing more than one carbon, and unsaturated hydrocarbon chains (C_6-C_9). Cyclopentenones may form as sodium muconate cleaves to form sodium carbonate and a five-carbon ring. Increasing sodium formate concentration with black liquor pre-treatment, or addition of excess formate prior to TDO has the potential to increase the volatile matter that can be condensed into a liquid hydrocarbon product. The volatile matter will contain highly deoxygenated compounds; oxygenated compounds generally only contain one oxygen. At approximately 550°C, the relative abundance of benzenes substituted with hydrocarbon chains, especially toluenes, increases as cyclopentanones and cyclopentenones decrease. The optimal operating temperature for fast pyrolysis of sodium muconate/formate mixutres is approximately 500°C. Solid products remaining after TDO are assumed to be carbonaceous material and sodium carbonate. Further repeatable analyses of sodium concentration in the product remaining after oxidation are necessary.

Neutralized muconic acid and formic acid serve as model compounds for the thermochemical conversion of oxidized black liquor. The results of this project can be used to better understand current and future research on black liquor TDO, as products seen in micro-scale fast pyrolysis may be seen in liquid hydrocarbons obtained through thermochemical conversion.

Proposed Future Work

As already proposed, further sodium analyses using sodium concentration and TIC should be performed to understand and quantify sodium carbonate in the product after

pyrolysis and oxidation. Additional trials at 550°C for sodium muconate and the muconate/formate mixture should be carried out to gather more product distribution data and analyze the experimental sodium carbonate mass after oxidation.

Overall product distribution analysis could be continued using alkane standards and retention indices (RI) in the GC/MS. If alkane standards were injected into the GC/MS, retention times specific to the equipment used in these experiments would be determined for a variety of hydrocarbon chains. Retention indices provide a means to convert the alkane retention times into constant values. RI and retention time data obtained in these experiments could be compared to the retention times and matches given by the GC/MS software to determine the accuracy of the data.

Cis-cis-muconic acid should be studied to determine the effects of stereochemistry on product distribution and reaction pathway. It can be synthesized from glucose and further converted as a platform chemical for bio-plastics. If the *cis-cis* isomer becomes a more valuable compound in the future, it may be prudent to study its potential hydrocarbon products.

Calcium, potassium and magnesium muconate and muconate/formate salts were also synthesized. These should also undergo Py-GC/MS analysis, especially calcium, which can be recycled in a chemical pulp mill in a similar process as sodium. There may be a difference between the effect of monovalent and divalent cations in thermal deoxygenation. Further Py-GC/MS would quantify differences and similarities.

References

(1) U.S. Energy Information Administration. Short-Term Energy Outlook: U.S. Crude Oil and Liquid Fuels. Feb 12, 2013. Accessed March 8, 2013. http://www.eia.gov/forecasts/steo/report/us_oil.cfm

(2) Schwartz, T. J.; van Heiningen, A. R. P.; Wheeler, M. C., Energy densification of levulinic acid by thermal deoxygenation. *Green Chemistry* **2010**, *12*, 1353-1356.

(3) Nowakowski, D. J.; Bridgwater, A. V.; Elliott, D. C.; Meier, D.; de Wild, P., Lignin fast pyrolysis: Results from an international collaboration. *Journal of Analytical and Applied Pyrolysis* **2010**, *88*, 53-72.

(4) Brebu, M.; Vasile, C., Thermal degradation of lignin – a review. *Cellulose Chemistry and Technology* **2009**, 353-363.

(5) Perlack, R. D.; Wright, L. L.; Turhollow, A. F.; Graham, R. L.; Stokes, B. J.; Erback, D. J., Biomass as a Feedstock for a Bioenergy and Bioproducts Industry: The Technical Feasibility of a Billon-Ton Annual Supply. US Department of Energy: Oak Ridge, TN, 2005.

(6) Niemela, K.; Alen, R., Characterization of pulping liquors. *Analytical Methods in Wood Chemistry, Pulping and Papermaking* **1999**, Berlin, Springer.

(7) Polen, T.; Spelberg, M.; Bott, M., Toward biotechnological production of adipic acid and precursors from biorenewables, *Journal of Biotechnology*, **2012**, Online.

(8) Curran, K. A.; Leavitt, J. M.; Karim, A. S.; Alper, H. S., Metabolic engineering of muconic acid production in *Saccharomyces cerevisiae*. *Metabolic Engineering*

2013, *15*, 55-67.

(9) Marinova, M.; Mateos-Espejel, E.; Jemaa, N.; Paris, J., Addressing the increased energy demand of a Kraft mill biorefinery: The hemicellulose extraction case, Chemical Engineering Research and Design **2009**, *87*, 1269-1275. Accessed March 7, 2013. http://www.sciencedirect.com/science/article/pii/S0263876209001531

(10) Gellerstedt, G.; Lindfors, E.-L., On the structure and reactivity of residual lignin in kraft pulp fibers. *Proceedings of the international pulp bleaching conference*, Stockholm, 11-14 June 1991, 73-88.

(11) Smook, G. *Handbook for pulp & paper technologists (2nd ed.)*. Bellingham, WA: Angus Wilde, 1992.

(12) Kalliola, A.; Kuitunen, S.; Liitia, T.; Rovio, S.; Ohra-aho, T.; Vuorinen, T.; Tamminen, T., Lignin oxidation mechanisms under oxygen delignification conditions. Part 1.Results from direct analyses. *Holzforschung* **2011**, *65*, 567-574.

(13) Kuitunen, S.; Kalliola, A.; Tarvo, V.; Tamminen, T.; Rovio, S.; Littia, T.; Ohra-aho, T.; Lehtimaa, T.; Vuorinen, T.; Alopaeus, V., Lignin oxidation mechanisms under oxygen delignification conditions. Part 3. Reaction pathways and modeling. *Holzforschung* **2011**, *65*, 587-599.

(14) Case, P. A.; van Heiningen, A. R. P.; Wheeler, M. C., Liquid hydrocarbon fuels from cellulosic feedstocks via thermal deoxygenation of levulinic acid and formic acid salt mixtures. *Green Chemistry* **2012**, *14*, 85-89.

(15) Mukkamala, S.; Wheeler, M. C.; van Heiningen, A. R. P.; DeSisto, W. J., Formate-Assisted Fast Pyrolysis of Lignin. *Energy & Fuels* **2012**, *26*, 1380-1384.

(16) Hayes, D. J.; Ross, J.; Hayes, M. H. B.; Fitzpatrick, S., The Biofine Process: Production of Levulinic Acid, Furfural and Formic Acid from Lignocellulosic Feedstocks. Carbolea. 2005. Accessed March 8, 2013.

(17) McMaster, M. and McMaster, C. *GC/MS: A Practical User's Guide*; Wiley-VCH: New York, 1998.

(18) Reed, R, Jr. Novel method for production of hydrogen and hydrogen-carbon monoxide mixtures. U. S. Patent 4,087,373, 1978.

Appendices

Appendix A

Salt Synthesis Tables

Table A1. Preparation of sodium muconate used for fast pyrolysis and GC/MS analysis.

Na Muconate - Sample 1				
Solution	Compound	Mass (mg)	Volume (mL)	Moles (mmol)
A1	Muconic Acid	142.3	-	1.002
	Ethanol	789.0	1.00	17.13
A2	Sodium Hydroxide	104.5	-	2.613
	DI Water	2613	2.61	145.2
A	A1 + A2	3649	3.61	165.9
Dry Mixture	C (Dry)	179.9	-	

Table A2. Preparation of sodium muconate/formate used for fast pyrolysis and GC/MS analysis.

Na Muconate/Formate - Sample 20				
Solution	Compound	Mass (mg)	Volume (mL)	Moles (mmol)
A1	Muconic Acid	142.3	-	1.002
	Ethanol	789.0	1.00	17.13
A2	Sodium Hydroxide	893.0	-	22.34
	DI Water	5000	5.00	277.8
A	A1 + A2	6824	6.00	318.2
B	Sodium Formate	136.3	-	2.004
	DI Water	1000	1.00	55.56
C	A+B	14785	13.00	694.1
Dry Mixture	C (Dry)	311.8	-	

Appendix B

Thermogravimetric Analysis Plots

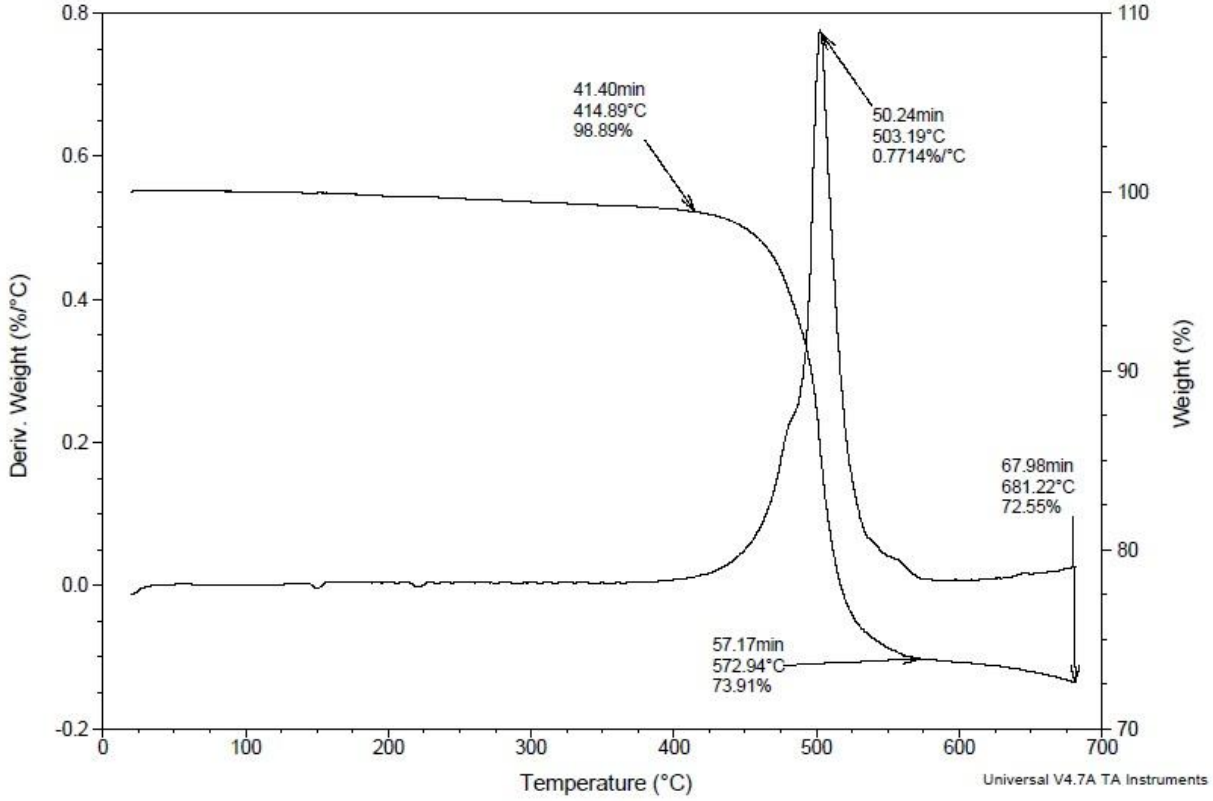

Figure B1. Slow pyrolysis of sodium muconate in a TGA with decomposition peaks indicated. TGA temperature was ramped 10°C/min from 20°C to 700°C. N_2 was used as the sweep gas.

Appendix C

Mass Measurement Data for Blanks

Table C1. Mass measurements of empty quartz tubes after pyrolysis.

Trial	Temperature (°C)	Mass Difference After Pyrolysis (%)
Blank Tube 1	500	0.037296
Blank Tube 2	450	0.018655
Blank Tube 3	500	0.046637
Blank Tube 4	450	0.018657
Blank Tube 550 1	550	0.036795
Blank Tube 550 5	550	-0.018957

Table C2. Mass measurements of quartz tubes stuffed with quartz wool after pyrolysis and oxidation.

Trial	Temperature (°C)	Overall Mass Difference After Oxidation (%)
Blank Tube 3	500	0.0093275
Blank Tube 4	450	0.00000
Blank Tube Wool 3	500	0.15500
Blank Tube Wool 4	450	0.18357
Blank Tube Wool 550 3	550	0.25028
Blank Tube Wool 550 4	550	0.25246
Blank Tube 550 1	550	0.0183976
Blank Tube 550 5	550	0.0094787

Appendix D

Trial Record and Mass Balances

Table D1. Sodium muconate trial mass measurements and balances.

Salt	Na Muconate	Na Muconate	Na Muconate	Na Muconate	Na Muconate	Na Muconate
Temperature (°C)	450	450	500	500	550	550
Trial No.	17	18	13	19	22	24
Mass of salt (mg)	1.76	2.08	1.29	1.67	1.28	1.4
Salt Mass Volatilized (%)	14.0	11.8	27.8	25.4	18.2	19.6
Mass lost after oxidation (mg)	0.76	0.91	0.31	0.49	0.41	0.48
Mass lost after oxidation (% of salt mass)	43.2	43.8	24.0	29.3	32.0	34.3
Experimental Sodium Carbonate Mass (mg)	0.75	0.92	0.62	0.76	0.64	0.65
Experimental Sodium Carbonate Mass (%)	42.6	44.2	48.1	45.5	50.0	46.4
Theoretical Sodium Carbonate Mass (mg)	1.00	1.19	0.74	0.95	0.73	0.80
Theoretical Sodium Carbonate Mass (%)	57.0	57.0	57.0	57.0	57.0	57.0

Table D2. Sodium muconate/formate trial mass measurements and balances.

Salt	Na Muc/Form	Na Muc/Form	Na Muc/Form	Na Muc/Form	Na Muc/Form	Na Muc/Form
Temperature (°C)	450	450	500	500	550	550
Trial No.	11	12	10	13	16	17
Mass of salt (mg)	1.12	1.25	2.98	1.27	1.47	1.45
Salt Mass Volatilized (%)	21.3	20.9	31.1	28.8	21.5	19.7
Mass lost after oxidation (mg)	0.32	0.33	0.57	0.23	0.12	0.20
Mass lost after oxidation (% of salt mass)	28.6	26.4	19.1	18.1	8.2	13.8
Experimental Sodium Carbonate Mass (mg)	0.56	0.66	1.48	0.67	1.03	0.96
Experimental Sodium Carbonate Mass (%)	50.0	52.8	49.7	52.8	70.1	66.2
Theoretical Sodium Carbonate Mass (mg)	0.74	0.82	1.96	0.84	0.97	0.954
Theoretical Sodium Carbonate Mass (%)	65.8	65.8	65.8	65.8	65.8	65.8

Appendix E

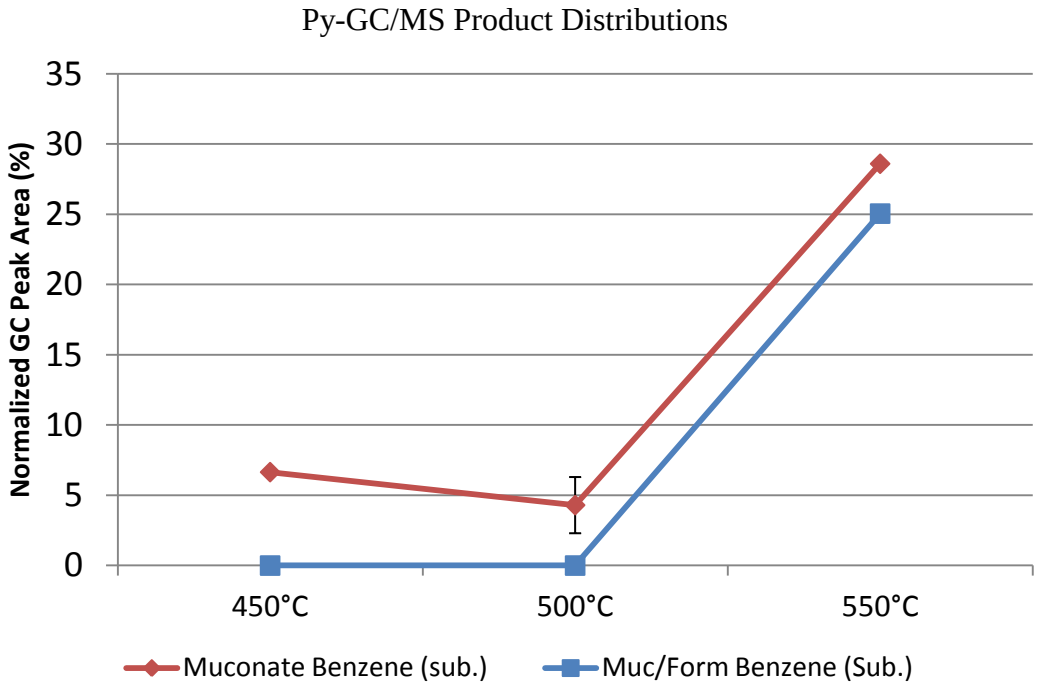

Figure E1. Product abundance trend for benzene compounds substituted with hydrocarbon chains containing more than one carbon in sodium muconate and sodium muconate/formate Py-GC/MS trials.

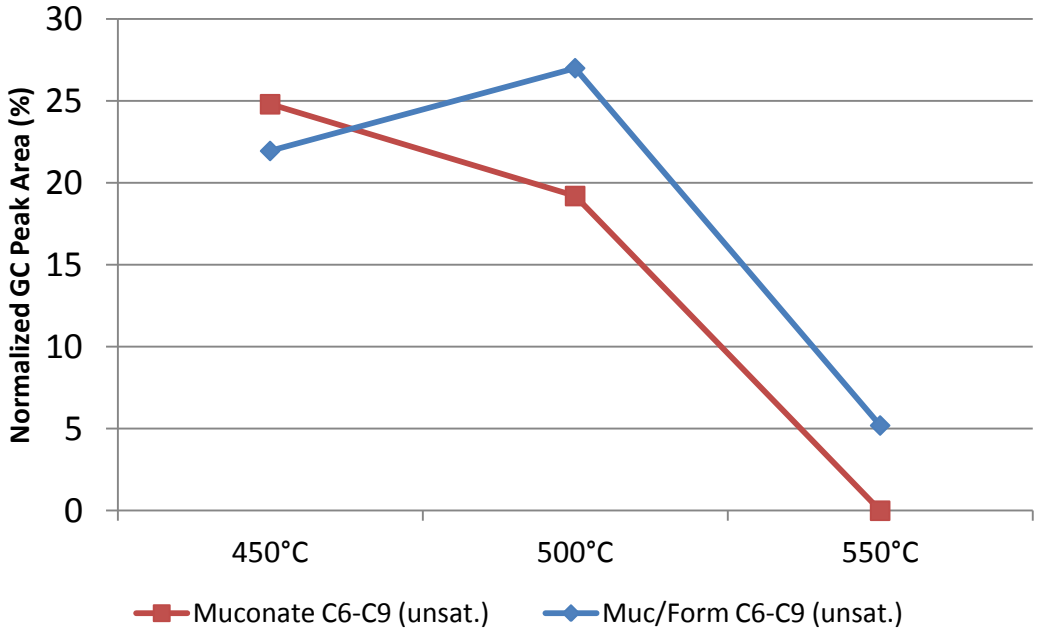

Figure E2. Product abundance trend for unsaturated hydrocarbon chains containing six to nine carbons in sodium muconate and sodium muconate/formate Py-GC/MS trials.

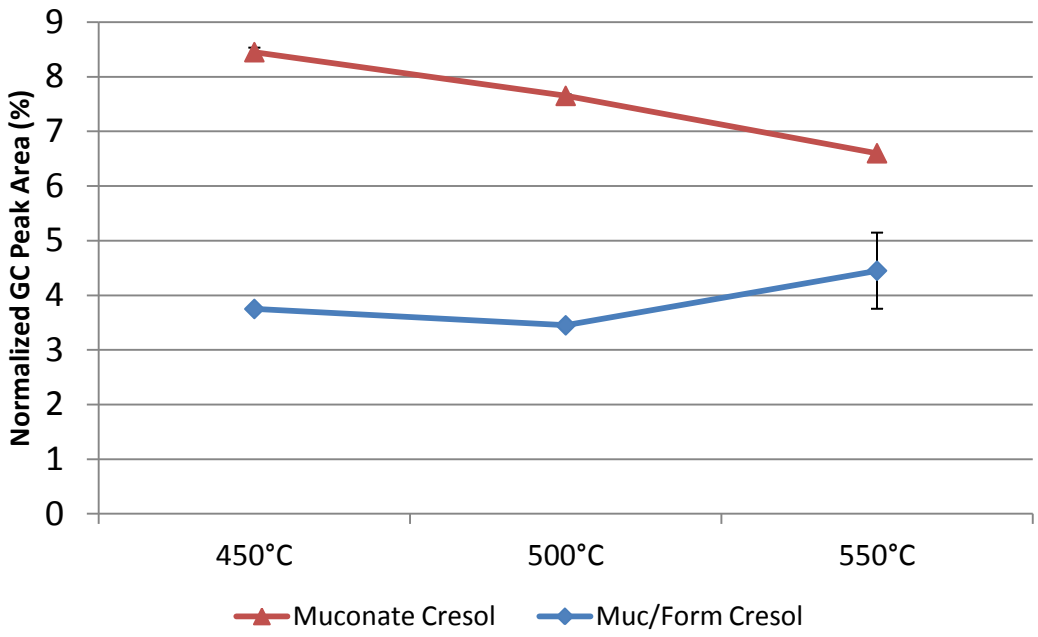

Figure E3. Product abundance trend for cresol in sodium muconate and sodium muconate/formate Py-GC/MS trials.

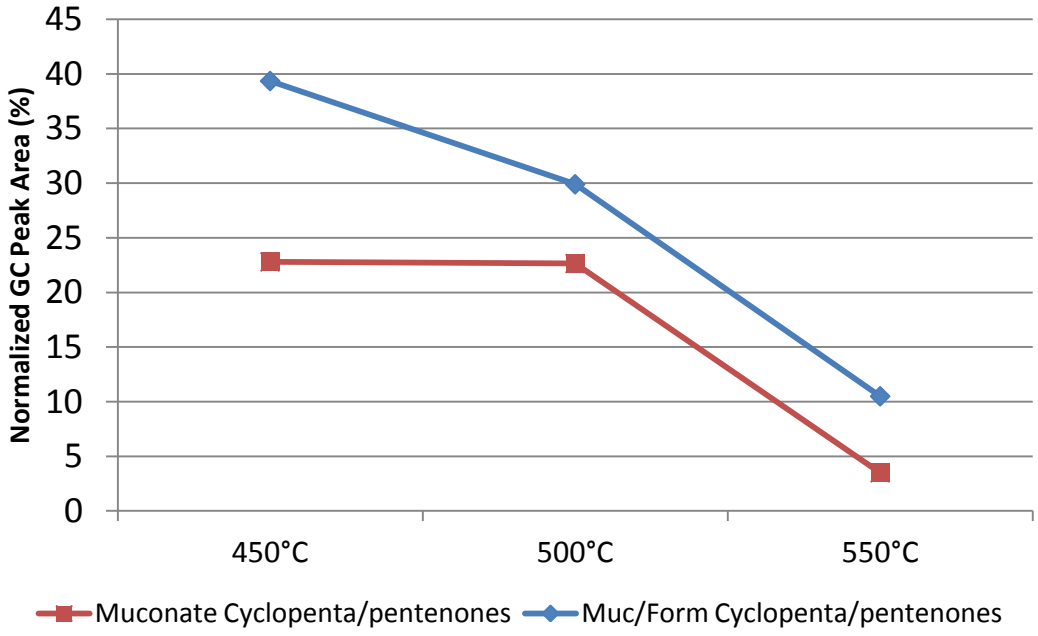

Figure E4. Product abundance trend for cyclopenta/pentenones in sodium muconate and sodium muconate/formate Py-GC/MS trials.

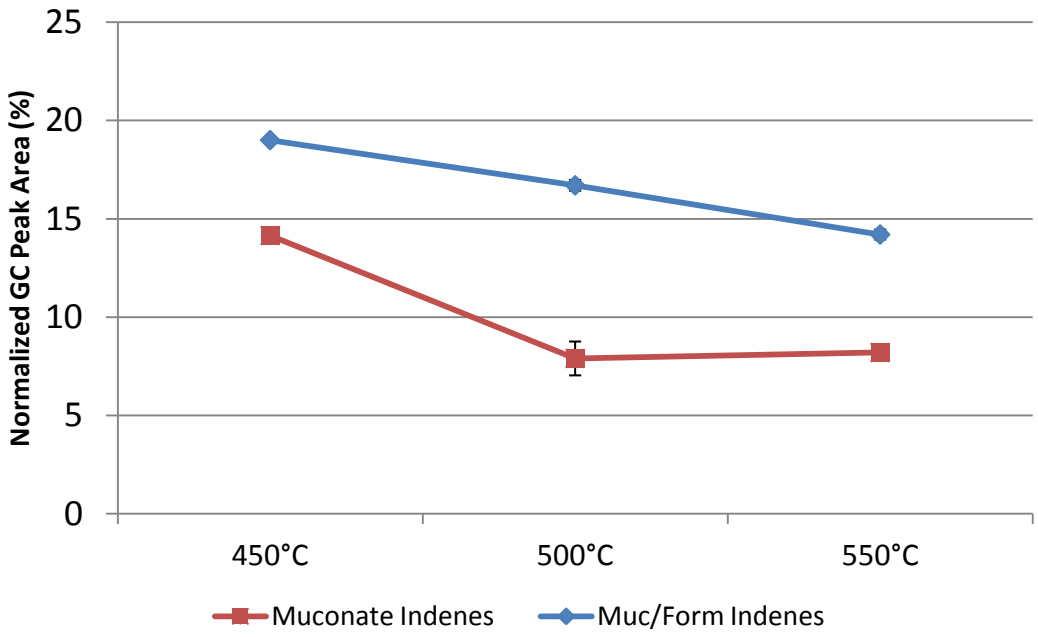

Figure E5. Product abundance trend for indenes, methylated indenes, and inden-1-ones in sodium muconate and sodium muconate/formate Py-GC/MS trials.

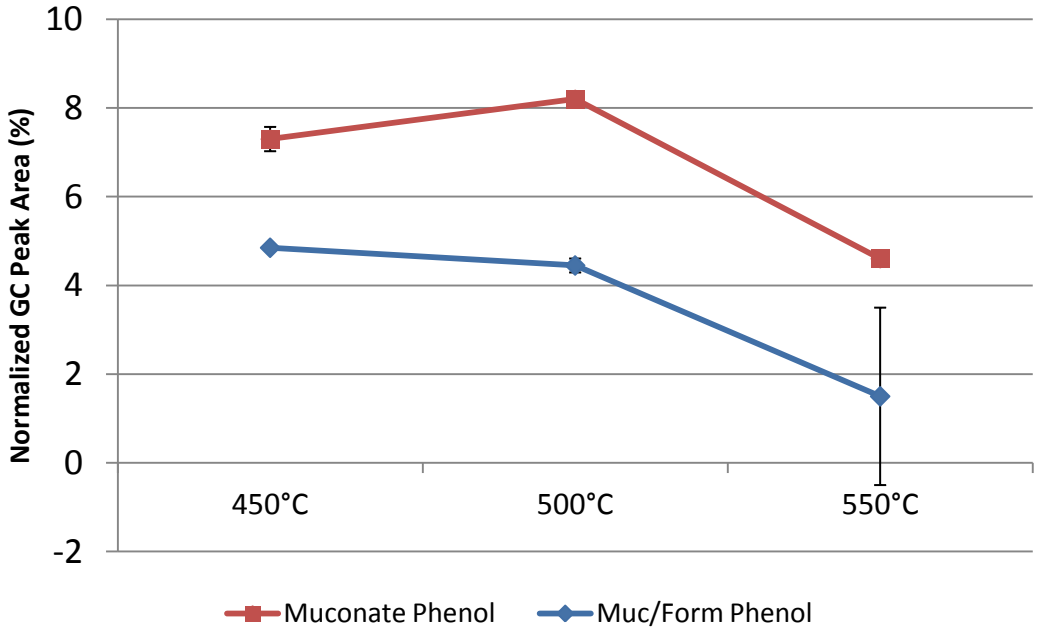

Figure E6. Product abundance trend for phenol in sodium muconate and sodium muconate/formate Py-GC/MS trials.

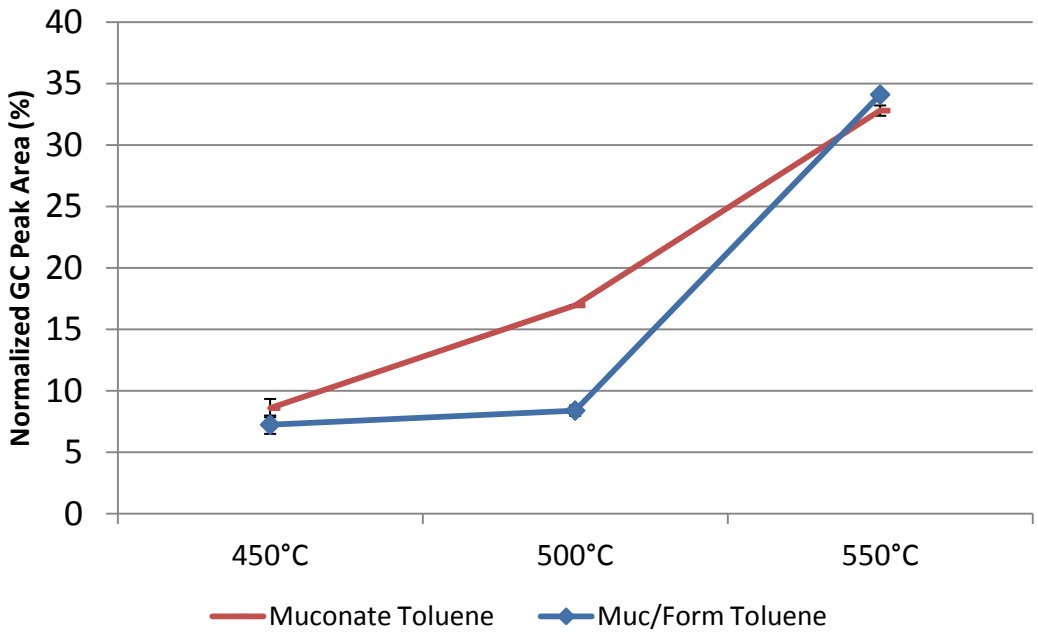

Figure E7. Product abundance trend for toluene in sodium muconate and sodium muconate/formate Py-GC/MS trials.

Appendix F

$$M_{Na} := 22.99 \frac{gm}{mol} \qquad M_C := 12.01 \frac{gm}{mol} \qquad M_H := 1.01 \frac{gm}{mol} \qquad M_O := 15.999 \frac{gm}{mol}$$

Sodium Salts

$$M_{NaMuc} := 2M_{Na} + 6 \cdot M_C + 4 \cdot M_H + 4 \cdot M_O = 186.076 \cdot \frac{gm}{mol}$$

$$M_{NaForm} := M_{Na} + M_C + M_H + 2M_O = 68.008 \cdot \frac{gm}{mol}$$

$$M_{NaMucForm} := M_{NaMuc} + 2M_{NaForm} = 322.092 \cdot \frac{gm}{mol}$$

Portion of mixture that is muconate or formate

$$NaMix\_Muc := \frac{M_{NaMuc}}{M_{NaMucForm}} = 0.578$$

$$NaMix\_Form := \frac{2M_{NaForm}}{M_{NaMucForm}} = 0.422$$

Carbonate

$$M_{NaCarb} := 2M_{Na} + M_C + 3.M_O = 105.987 \cdot \frac{gm}{mol}$$

Conversions
Mass of salt –> moles of salt
Moles of salt –> Theoretical moles of carbonate
Theoretical moles of carbonate --> Theoretical mass of carbonate
How do the theoretical and experimental carbonate masses compare?

Maximum Theoretical Conversion

Percent by mass of the conversion of salt to sodium carbonate:

Na Muconate $\frac{M_{NaCarb}}{M_{NaMuc}} = 56.959 \cdot \%$

Na Muconate/Formate $\frac{2 \cdot M_{NaCarb}}{M_{NaMucForm}} = 65.812 \cdot \%$

450°C Trials

Na Muconate 17

$m_{NaMuc17} := (0.00176\,gm)$ Mass of original salt

$n_{NaMuc17} := \frac{m_{NaMuc17}}{M_{NaMuc}} = 9.459 \times 10^{-6}\,mol$ Moles of original salt

$n_{NaCarb17} := n_{NaMuc17}$ Theoretical moles of sodium carbonate
For Na muconates, there is a 1 salt:1 carbonate ratio.

$m_{NaCarb17} := n_{NaCarb17} \cdot M_{NaCarb} = 1.002 \cdot mg$ Theoretical mass of sodium carbonate

Conversion:

$\frac{m_{NaCarb17}}{m_{NaMuc17}} = 57.0 \cdot \%$

Na Muconate 18

$m_{NaMuc18} := 0.00208\,gm$

$n_{NaMuc18} := \frac{m_{NaMuc18}}{M_{NaMuc}} = 1.118 \times 10^{-5}\,mol$

$n_{NaCarb18} := n_{NaMuc18}$ For Na muconates, there is a 1 salt:1 carbonate ratio.

$m_{NaCarb18} := n_{NaCarb18} \cdot M_{NaCarb} = 1.185 \cdot mg$

Conversion:

$\frac{m_{NaCarb18}}{m_{NaMuc18}} = 57.0 \cdot \%$

450°C Trials Continued

Na Muconate/Formate 11

$m_{NaMucForm11} := (0.00112\,gm)$

$n_{NaMucForm11} := \frac{m_{NaMucForm11}}{M_{NaMucForm}} = 3.477 \times 10^{-6}\,mol$

$n_{NaCarb11} := 2 n_{NaMucForm11}$ For Na muconate/formate, there is a 1 salt:2 carbonate ratio.

$m_{NaCarb11} := n_{NaCarb11} \cdot M_{NaCarb} = 0.737 \cdot mg$

Conversion:

$$\frac{m_{NaCarb11}}{m_{NaMucForm11}} = 65.8 \cdot \%$$

Na Muconate/Formate 12

$m_{NaMucForm12} := 0.00125\,gm$

$n_{NaMucForm12} := \frac{m_{NaMucForm12}}{M_{NaMucForm}} = 3.881 \times 10^{-6}\,mol$

$n_{NaCarb12} := 2 n_{NaMucForm12}$ For Na muconate/formate, there is a 1 salt:2 carbonate ratio.

$m_{NaCarb12} := n_{NaCarb12} \cdot M_{NaCarb} = 0.823 \cdot mg$

Conversion:

$$\frac{m_{NaCarb11}}{m_{NaMucForm11}} = 65.8 \cdot \%$$

500°C Trials

Na Muconate 13

$m_{NaMuc13} := 0.00129\,gm$

$n_{NaMuc13} := \frac{m_{NaMuc13}}{M_{NaMuc}} = 6.933 \times 10^{-6}\,mol$

$n_{NaCarb13} := n_{NaMuc13}$ For Na muconates, there is a 1 salt:1 carbonate ratio.

$m_{NaCarb13} := n_{NaCarb13} \cdot M_{NaCarb} = 0.735 \cdot mg$

Conversion:

$\frac{m_{NaCarb13}}{m_{NaMuc13}} = 57.0 \cdot \%$

Na Muconate 19

$m_{NaMuc19} := 0.00167\,gm$

$n_{NaMuc19} := \frac{m_{NaMuc19}}{M_{NaMuc}} = 8.975 \times 10^{-6}\,mol$

$n_{NaCarb19} := n_{NaMuc19}$ For Na muconates, there is a 1 salt:1 carbonate ratio.

$m_{NaCarb19} := n_{NaCarb19} \cdot M_{NaCarb} = 0.951 \cdot mg$

Conversion:

$\frac{m_{NaCarb19}}{m_{NaMuc19}} = 57.0 \cdot \%$

500°C Trials Continued

Na Muconate/Formate 10

$m_{NaMucForm10} := 0.00298\,gm$

$n_{NaMucForm10} := \frac{m_{NaMucForm10}}{M_{NaMucForm}} = 9.252 \times 10^{-6}\,mol$

$n_{NaCarb10} := 2 n_{NaMucForm10}$ For Na muconate/formate, there is a 1 salt:2 carbonate ratio.

$m_{NaCarb10} := n_{NaCarb10} \cdot M_{NaCarb} = 1.961 \cdot mg$

Conversion: $\frac{m_{NaCarb10}}{m_{NaMucForm10}} = 65.8 \cdot \%$

Na Muconate/Formate 13

$m_{NaMucForm13} := 0.00127\,gm$

$n_{NaMucForm13} := \frac{m_{NaMucForm13}}{M_{NaMucForm}} = 3.943 \times 10^{-6}\,mol$

$n_{NaCarb13} := 2 n_{NaMucForm13}$ For Na muconate/formate, there is a 1 salt:2 carbonate ratio.

$m_{NaCarb13} := n_{NaCarb13} \cdot M_{NaCarb} = 0.836 \cdot mg$

Conversion: $\frac{m_{NaCarb13}}{m_{NaMucForm13}} = 65.8 \cdot \%$

550°C Trials

Na Muconate 22

$m_{NaMuc22} := 0.00128\,gm$

$n_{NaMuc22} := \frac{m_{NaMuc22}}{M_{NaMuc}} = 6.879 \times 10^{-6}\,mol$

$n_{NaCarb22} := n_{NaMuc22}$ For Na muconates, there is a 1 salt:1 carbonate ratio.

$m_{NaCarb22} := n_{NaCarb22} \cdot M_{NaCarb} = 0.729 \cdot mg$

Conversion:

$\frac{m_{NaCarb22}}{m_{NaMuc22}} = 57.0 \cdot \%$

Na Muconate 24

$m_{NaMuc24} := 0.00140\,gm$

$n_{NaMuc24} := \frac{m_{NaMuc24}}{M_{NaMuc}} = 7.524 \times 10^{-6}\,mol$

$n_{NaCarb24} := n_{NaMuc24}$ For Na muconates, there is a 1 salt:1 carbonate ratio.

$m_{NaCarb24} := n_{NaCarb24} \cdot M_{NaCarb} = 0.797 \cdot mg$

Conversion:

$\frac{m_{NaCarb19}}{m_{NaMuc19}} = 57.0 \cdot \%$

550°C Trials Continued

Na Muconate/Formate 16

$m_{NaMucForm16} := 0.00147\,gm$

$n_{NaMucForm16} := \frac{m_{NaMucForm16}}{M_{NaMucForm}} = 4.564 \times 10^{-6}\,mol$

$n_{NaCarb16} := 2 n_{NaMucForm16}$ For Na muconate/formate, there is a 1 salt:2 carbonate ratio.

$m_{NaCarb16} := n_{NaCarb16} \cdot M_{NaCarb} = 0.967 \cdot mg$

Conversion: $\frac{m_{NaCarb10}}{m_{NaMucForm10}} = 65.8 \cdot \%$

Na Muconate/Formate 17

$m_{NaMucForm17} := 0.00145\,gm$

$n_{NaMucForm17} := \frac{m_{NaMucForm17}}{M_{NaMucForm}} = 4.502 \times 10^{-6}\,mol$

$n_{NaCarb17} := 2 n_{NaMucForm17}$ For Na muconate/formate, there is a 1 salt:2 carbonate ratio.

$m_{NaCarb17} := n_{NaCarb17} \cdot M_{NaCarb} = 0.954 \cdot mg$

Conversion: $\frac{m_{NaCarb17}}{m_{NaMucForm17}} = 65.8 \cdot \%$

Appendix G

Sodium Content in Na Muconate and Na Muconate/Formate Samples after Pyrolysis & Oxidation

Molar Masses

$M_{Na} := 22.99\frac{gm}{mol}$ $M_C := 12.01\frac{gm}{mol}$ $M_H := 1.01\frac{gm}{mol}$ $M_O := 15.999\frac{gm}{mol}$

$M_{NaOH} := M_{Na} + M_O + M_H = 39.999\frac{gm}{mol}$ Sodium hydroxide

$M_{NaCarb} := 2M_{Na} + M_C + 3 \cdot M_O = 105.987\frac{gm}{mol}$ Sodium carbonate

$M_{Na2} := 2 \cdot M_{Na} = 45.98\frac{gm}{mol}$ Sodium in sodium carbonate

Mass of Analyzed Sample
(Sample after oxidation, filtering, dissolving in 0.1 M HCl, and drying)

Na Muconate 19 $m_{NaM19} := 0.72mg$

Na Muconate/Formate 13 $m_{NaMF13} := 0.67mg$

Data from the Department of Plant, Soil and Environmental Sciences

"Residue was dissolved in ddH2O and analyzed by ICPOES"

$ppm := 10^{-6}$ $\rho := 1.0\frac{gm}{mL}$ Assumed density of water

Na Muconate 19 $C_{NaM19} := 65.0ppm$ $Volume_{NaM19} := 5.0mL$

Na Muconate/Formate 13 $C_{NaMF13} := 77.8ppm$ $Volume_{NaMF13} := 5.0mL$

Sodium Masses After Oxidation

Na Muconate 19

$$m_{Na\_NaM19} := C_{NaM19} \cdot Volume_{NaM19} \cdot \rho$$

$$m_{Na\_NaM19} = 0.33 \cdot mg$$

Sodium in sample after oxidation

$$\frac{m_{Na\_NaM19}}{m_{NaM19}} = 45.1 \cdot \%$$

Na Muconate/Formate 13

$$m_{Na\_NaMF13} := C_{NaMF13} \cdot Volume_{NaMF13} \cdot \rho$$

$$m_{Na\_NaMF13} = 0.39 \cdot mg$$

Sodium in sample after oxidation

$$\frac{m_{Na\_NaMF13}}{m_{NaMF13}} = 58.1 \cdot \%$$

Theoretical Mass of Sodium Carbonate in the Sample, According to Concentration

Na Muconate 19

$$m_{TheoNaCarb\_NaM19} := m_{Na\_NaM19} \cdot \frac{M_{NaCarb}}{M_{Na2}}$$

There are 2 sodium atoms in 1 sodium carbonate.

$$m_{TheoNaCarb\_NaM19} = 0.75 \cdot mg$$

Na Muconate/Formate 13

$$m_{TheoNaCarb\_NaMF13} := m_{Na\_NaMF13} \cdot \frac{M_{NaCarb}}{M_{Na2}}$$

$$m_{TheoNaCarb\_NaMF13} = 0.90 \cdot mg$$

Author Biography

Laura Duran was born in Falmouth, ME. She attended Falmouth Public Schools, Catherine McAuley High School, and will graduate from The University of Maine in May 2013. She studied chemical engineering as a University of Maine Pulp & Paper Foundation Scholar. In her time at the University, she competed in Division I Women's Swimming, worked as a student ambassador for New Student Programs, and participated in engineering and honor societies, including All Maine Women and Tau Beta Pi. She plans to work at Verso Paper Corp. – Bucksport Mill as a process engineer after graduation.